



Importance of L-selectin in the induction of immune responses in the upper respiratory tract
by Keri Lin Csencsits

A dissertation submitted in partial fulfillment of the requirements for the degree of Doctor of
Philosophy in Veterinary Molecular Biology
Montana State University
© Copyright by Keri Lin Csencsits (2001)

Abstract:

Recent evidence suggests that the “common mucosal immune system” (CMIS) is, in fact, compartmentalized. Intranasal (i.n.) immunization preferentially induces effector immune responses in the nasal passages (NP) and reproductive tract (RT), while oral immunization induces robust intestinal response, and little to no response in NP or RT. Furthermore, intestinal mucosal addressin cell adhesion molecule-1 (MAdCAM-1) - $\alpha 4\beta 7$ homing interactions do not appear to be important for the induction of immunity after i.n. immunization. Therefore, we hypothesized that L-selectin-peripheral node addressin (PNAd) interactions are important for induction of immune responses in the NP and RT. Identification of addressins on naive nasal associated tissue (NALT) and cranial, oral and nasal associated tissue (CONALT) revealed that these sites express primarily PNAd, rather than MAdCAM-1, and that naive lymphocyte binding is mediated through L-selectin-PNAd interactions. In fact, NALT and CONALT more closely resemble peripheral lymph node (PLN) than the intestinal mucosal inductive site, the Peyer’s patch (PP). Studies of addressin expression in NALT after i.n. cholera toxin (CT) immunization revealed increase in expression and functionality of MAdCAM-1 on HEV as well as MAdCAM-1 expression by dendritic cells (DC). Studies of effector immune responses in L-selectin-deficient ($L\text{-Sel}^{-/-}$) mice revealed that Ab responses in NP and RT, but not intestinal lamina propria (iLP) were abated 16 days post-i.n. CT immunization. Investigation of lymphocyte homing receptors revealed that an $L\text{-selectin}^{\text{low}}/\beta 7^{\text{low}}(\alpha 4\beta 7^{\text{+}})$ B lymphocyte population provides effector immunity in NP and RT, while iLP effector immune response is contained within the $L\text{-selectin}^{\text{low}}/\beta 7^{\text{low}}(\alpha 4\beta 7^{\text{+}})$ B lymphocyte subpopulation as well as a unique $L\text{-selectin}^{\text{low}}/\beta 7^{\text{high}}(\alpha E^{\text{+}})$ B lymphocyte population that is unaffected by the loss of L-selectin. Moreover, oral immunization of $L\text{-Sel}^{-/-}$ mice induced response in all effector sites, and increased response in CONALT suggesting a definite difference in the effect of loss of L-selectin on inductive immune responses in PP. Finally, long-term immunization studies revealed that effector immune responses in $L\text{-Sel}^{-/-}$ NP and RT are delayed, not eliminated, and Ab response was significantly increased in $L\text{-Sel}^{-/-}$ CONALT. Together, these results highlight the important of L-selectin-PNAd homing interactions in induction of immunity after i.n. immunization, and support the concept of the compartmentalization of the CMIS.

IMPORTANCE OF L-SELECTIN IN THE INDUCTION OF IMMUNE RESPONSES
IN THE UPPER RESPIRATORY TRACT

by

Keri Lin Csencsits

A dissertation submitted in partial fulfillment
of the requirements for the degree

of

Doctor of Philosophy

in

Veterinary Molecular Biology

MONTANA STATE UNIVERSITY
Bozeman, MT

November 2001

© COPYRIGHT

by

Keri Lin Csencsits

2001

All Rights Reserved

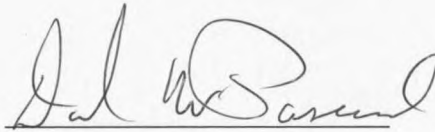
D378
C89

APPROVAL

of a dissertation submitted by

This dissertation has been read by each member of the dissertation committee and has been found to be satisfactory regarding content, English usage, format, citations, bibliographic style, and consistency, and is ready for submission to the College of Graduate Studies.


David W. Pascual



12/6/01
Date

Approved for the Department of Veterinary Molecular Biology

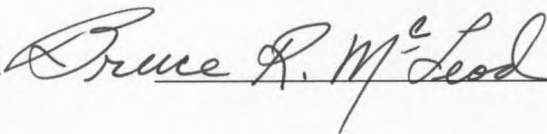
Allen G. Harmsen



12/7/01
Date

Approved for the College of Graduate Studies

Bruce R. McLeod



12-10-01
Date

STATEMENT OF PERMISSION TO USE

In presenting this dissertation in partial fulfillment of the requirements for a doctoral degree at Montana State University, I agree that the Library shall make it available to borrowers under rules of the Library. I further agree that copying of this dissertation is allowable only for scholarly purposes, consistent with "fair use" as prescribed in the U. S. Copyright Law. Requests for extensive copying or reproduction of this dissertation should be referred to Bell & Howell Information and Learning, 300 North Zeeb Road, Ann Arbor, Michigan 48106, to whom I have granted "the exclusive right to reproduce and distribute my dissertation in and from microform along with the non-exclusive right to reproduce and distribute my abstract in any format in whole or in part."

Signature Kari J. Coons

Date 12/6/01

ACKNOWLEDGEMENTS

I would like to thank my committee members
Dr. Mark Jutila, Dr. Michele Hardy, and Dr. Clifford Bond
for their time and suggestions throughout the course of this research.

I would also like to thank Dr. David Pascual for his financial support, guidance, and
encouragement

Finally, I would like to thank Christopher N. Smith.
Who has more than made up for the 3 AM poster session.

TABLE OF CONTENTS

List of Tables	ix
List of Figures	x
Abstract	xiii
1. LYMPHOCYTE HOMING AND THE COMMON MUCOSAL IMMUNE SYSTEM	1
Mucosal Immunology	1
The common mucosal immune system.....	1
Compartmentalization of the common mucosal immune system	2
The mucosal immune system consists of inductive and effector sites.....	3
NALT is an inductive site for the nasal passages.....	6
Role of CONALT in the induction of nasal immunity	8
Lymphocyte Homing	10
Lymphocytes display specific trafficking pattern.....	10
The multistep model of lymphocyte homing	11
Addressin expression is tissue specific	12
Lymphocyte homing receptors	13
$\alpha_E\beta_7$ is an intestine-specific integrin.....	14
Expression of addressins by follicular dendritic cells may contribute to lymphocyte recruitment and retention	15
Different homing receptor-addressin pairs mediate memory lymphocyte homing to peripheral and mucosal sites.....	16
Roles of L-selectin and $\alpha_4\beta_7$ in memory B lymphocyte homing.....	17
Statement of the hypothesis	19
2. MATERIALS AND METHODS.....	21
Mice	21
Immunizations.....	21
Collection of serum, fecal, and vaginal samples.....	22
Anti-CT-B ELISA.....	22
Tissue isolation and collection.....	23
NP lymphocyte isolation.....	24
Intestinal LP lymphocyte isolation	25
RT lymphocyte isolation.....	26
Double immunofluorescent staining for tissue addressins.....	26
Immunohistochemical staining of MAdCAM-1 and VCAM-1.....	27
Blocking of lymphocyte adhesion to HEV	27
Comparison of $\alpha_4\beta_7$ and L-selectin expression on lymphocytes.....	28
<i>In vivo</i> lymphocyte homing	29
Flow cytometry and sorting of effector lymphocytes.....	31

CT-B-specific ELISPOT	31
Statistical analysis	32
3. NASAL-ASSOCIATED LYMPHOID TISSUE: PHENOTYPIC AND FUNCTIONAL EVIDENCE FOR THE PRIMARY ROLE OF PERIPHERAL NODE ADDRESSIN IN NAIVE LYMPHOCYTE ADHESION TO HIGH ENDOTHELIAL VENULES IN A MUCOSAL SITE	33
Introduction.....	33
Results and Discussion	36
Murine NALT HEV express a unique addressin profile	36
Initial naive lymphocyte binding to NALT HEV is mediated primarily by PNA _D -L-selectin interactions.....	39
NALT lymphocytes express a unique L-selectin profile	43
Segregation of double positive and PNA _D positive NALT HEV in B and T cell areas	44
Murine NALT is a unique mucosal inductive site	46
4. MAdCAM-1 EXPRESSION NAIVE LYMPHOCYTE BINDING INTERACTIONS VARY AMONG THE CONALT	53
Introduction.....	53
Results and Discussion	56
The CONALT display different addressin phenotypes	56
Extravascular MAdCAM-1 and VCAM-1 are expressed within CONALT	57
Naive lymphocyte binding to HEV of CONALT is mediated primarily by PNA _D -L-selectin interactions.....	59
Lymphocytes of the CONALT express primarily L-selectin	63
L-selectin primarily mediates in vivo homing of CONALT Lymphocytes.....	66
Implications of variable expression of MAdCAM-1 among CONALT	72
5. MAdCAM-1 EXPRESSION IS INCREASED ON HEV AND DENDRITIC CELLS OF CT IMMUNIZED NALT	77
Introduction.....	78
Results and Discussion	79
The percentage of HEV expressing MAdCAM-1 is increased in CT- immunized NALT	79
Increased MAdCAM-1 expressed by immunized NALT HEV is functional	81

Diffuse MAdCAM-1 staining correlates with N418 ⁺ DC staining.....	82
MAdCAM-1 expression on HEV and DC is dynamic.....	87
6. DICHOTOMY OF HOMING RECEPTOR DEPENDENCE BY MUCOSAL EFFECTOR B CELLS: α_E VS. L-SELECTIN.....	91.
Introduction.....	91
Results and Discussion	93
Vaginal, but not fecal or serum CT-B-specific IgA titers are reduced in CT-immunized L-Sel ^{-/-} mice.....	93
The iLP contains a unique subset of effector B lymphocytes.....	94
The L-selectin ^{low} / β_7 ^{low} B lymphocyte subset provides CT-B-specific responses in NP and RT	98
The L-selectin ^{low} / β_7 ^{high} ($\alpha_E\beta_7^+$) subset provides CT-B-specific and total IgA SFC in iLP	98
7. NON-INTESTINAL EFFECTOR RESPONSES ARE NOT REDUCED IN L-SELECTIN ^{-/-} MICE FOLLOWING ORAL IMMUNIZATION	103
Introduction	103
Results and Discussion	105
Oral immunization of L-Sel ^{-/-} mice induces AFC in NP, RT, and iLP ...	105
Effector B lymphocyte subsets induced by oral immunization are similar to those observed after nasal immunization.....	107
Ability of the L-selectin ^{low} / $\alpha_4\beta_7^+$ subset to induce immunity is not affected in orally immunized L-Sel ^{-/-} mice	108
LN cellularity is reduced in L-Sel ^{-/-} CONALT	112
AFC are increased in CONALT after oral CT immunization.....	112
Oral CT immunization stimulates unexpected immune responses in L-Sel ^{-/-} mice	114
8. EFFECTOR IMMUNE RESPONSES IN NON-INTESTINAL MUCOSAL EFFECTOR SITES IN L-SELECTIN ^{-/-} MICE ARE DELAYED, NOT ELIMINATED.....	119
Introduction.....	119
Results and Discussion	121
Loss of effector immune response in i.n. immunized L-Sel ^{-/-} mice is not due to loss of inductive site Ab production	121
Total IgA response is increased in L-Sel ^{-/-} CONALT in i.n. immunized mice.....	123

Immune responses are restored in L- $\text{Sel}^{-/}$ NP and RT by six weeks post-immunization	124
L-selectin ^{low} and $\alpha_4\beta_7^{\text{low}}$ lymphocytes are present in effector sites at 6 weeks post-immunization	129
CT-B-specific and total immune responses are increased in L- $\text{Sel}^{-/}$ CONALT.....	132
An $\alpha_E\beta_7$ lymphocyte population may provide increased Ab-forming cells in L- $\text{Sel}^{-/}$ CONALT	133
SUMMARY	144
REFERENCES CITED.....	152
APPENDICES	172
APPENDIX A: LIST OF ABBREVIATIONS	173
APPENDIX B: LIST OF PUBLICATIONS	176

LIST OF TABLES

Table	Page
1. Monoclonal antibodies used in experiments.....	30
2. Percentages of MAdCAM-1, PNAd, and double positive HEV in NALT, PP, MLN, and PLN	37
3. Comparison of percentages of NALT, PP, PLN, and MLN B and T lymphocytes that express L-selectin	44
4. Locations of double and single positive HEV within NALT and PP	47
5. Percentages of MAdCAM-1, PNAd, and double positive HEV in PRLN, SMLN, and CLN.....	57
6. Comparison of percentages of B and T lymphocytes expressing L-selectin in the CONALT	65
7. Comparison of percentages of B and T lymphocytes expressing $\alpha_4\beta_7$ in the CONALT	66
8. Percentages of control Ab treated, donor GFP ⁺ lymphocytes found in mucosal and peripheral tissues 4 hours and 24 hours after injection.....	69
9. Increase in the number of HEV expressing MAdCAM-1 in CT-immunized NALT ...	80
10. Number of lymphocytes/mouse obtained from L-Sel ^{+/+} and L-Sel ^{-/-} CONALT at 16 days post-oral CT immunization.....	113
11. Number of lymphocytes/mouse obtained from L-Sel ^{+/+} and L-Sel ^{-/-} CONALT at 16 days post-i.n. CT immunization.....	123
12. Number of lymphocytes/mouse obtained from L-Sel ^{+/+} and L-Sel ^{-/-} CONALT at 16 days post-i.n. CT immunization.....	135

LIST OF FIGURES

Figure	Page
1. Structure of the Peyer's patch	5
2. Murine NALT HEV display an addressin phenotype different from PP, MLN, and PLN	38
3. An anti-PNAd Ab blocks initial naive lymphocyte binding to NALT HEV	41
4. An anti-L-selectin Ab blocks initial naive lymphocyte binding to NALT HEV	42
5. Expression profiles of L-selectin on NALT resemble PLN.....	45
6. The CLN have a more mucosal phenotype than the SMLN or PRLN	58
7. An anti-L-selectin Ab blocks initial naive lymphocyte binding to CONALT HEV	60
8. An anti-PNAd Ab blocks initial naive lymphocyte binding to the CONALT	62
9. L-selectin is expressed on the majority of CONALT lymphocytes.....	64
10. CONALT lymphocytes express primarily $\alpha_4\beta_7^{\text{low}}$	67
11. Treatment with anti-L-selectin Ab reduces lymphocyte homing and retention in CONALT	71
12. MAdCAM-1 expression is increased on HEV and in stromal cell areas in 10 day CT-immunized NALT	80
13. MEL 14 and MECA 79 mAbs have decreased blocking ability in 10 day CT- immunized NALT	83
14. The ability of MEL 14 and MECA 79 mAbs to block naive lymphocyte binding to immunized NALT HEV is decreased	83
15. Expression of MAdCAM-1 and SED DC appear in subepithelial dome region (SED) of 10 day CT-immunized NALT	85
16. Expression of MAdCAM-1 and DC appear in the SED region of 10 day CT- immunized NALT	85

17. N418 ⁺ DC co-localize with MAdCAM-1 staining in 10 day CT-immunized NALT	86
18. Vaginal and nasal, but not serum or fecal, CT-B-specific Ab responses are reduced in L-Sel ^{-/-} mice.....	95
19. Three distinct homing receptor phenotypes are displayed by lymphocytes in mucosal effector sites.....	97
20. Specific effector populations produce CT-B-specific and total Ab.....	100
21. Oral CT immunization induces AFC in NP and RT, as well as iLP.....	106
22. Three distinct homing receptor profiles are observed on B lymphocytes isolated from NP, RT, and iLP 16 days post-primary oral immunization	109
23. The L-selectin ^{low} / $\alpha_4\beta_7$ ⁺ B lymphocyte subset contains the majority of CT-B-specific and total AFC in orally immunized L-Sel ^{+/+} and L-Sel ^{-/-} mice	111
24. CT-B-specific and total IgA AFC, and total IgG AFC are increased in L-Sel ^{-/-} CONALT	115
25. Inductive immune responses are found in L-Sel ^{-/-} NALT and PP 16 days post-primary i.n. CT immunization	122
26. Total IgA AFC are increased in L-Sel ^{-/-} CONALT at 16 days post-i.n. CT immunization	125
27. $\alpha_4\beta_7$ expression is not increased on L-Sel ^{-/-} CONALT 16 days post-i.n. CT immunization	125
28. Ab responses in L-Sel ^{+/+} and L-Sel ^{-/-} mice as determined by ELISA from days 0-42 post-i.n. CT immunization.....	127
29. AFC responses are restored in L-Sel ^{-/-} NP and RT by 6 weeks post-i.n. CT immunization	128
30. $\alpha_4\beta_7$ ⁺ , but not $\alpha_4\beta_7$ ^{high} expression is observed on L-Sel ^{+/+} and L-Sel ^{-/-} NP, iLP, and RT 6 weeks post i.n. CT immunization.....	131
31. CT-B-specific and total AFC are increased in 6 week i.n. CT immunized L-Sel ^{-/-} CONALT	134

32. $\alpha_4\beta_7$ expression is not increased, but $\alpha_E\beta_7$ expression is increased on L-*SEL*^{-/-}
CONALT 6 weeks post i.n. CT immunization137

33. Differences in addressin and homing receptor expression contribute to the
compartmentalization of the CMIS.....150

ABSTRACT

Recent evidence suggests that the "common mucosal immune system" (CMIS) is, in fact, compartmentalized. Intranasal (i.n.) immunization preferentially induces effector immune responses in the nasal passages (NP) and reproductive tract (RT), while oral immunization induces robust intestinal response, and little to no response in NP or RT. Furthermore, intestinal mucosal addressin cell adhesion molecule-1 (MAdCAM-1) – $\alpha_4\beta_7$ homing interactions do not appear to be important for the induction of immunity after i.n. immunization. Therefore, we hypothesized that L-selectin-peripheral node addressin (PNAd) interactions are important for induction of immune responses in the NP and RT. Identification of addressins on naive nasal associated tissue (NALT) and cranial, oral and nasal associated tissue (CONALT) revealed that these sites express primarily PNAd, rather than MAdCAM-1, and that naive lymphocyte binding is mediated through L-selectin-PNAd interactions. In fact, NALT and CONALT more closely resemble peripheral lymph node (PLN) than the intestinal mucosal inductive site, the Peyer's patch (PP). Studies of addressin expression in NALT after i.n. cholera toxin (CT) immunization revealed increase in expression and functionality of MAdCAM-1 on HEV as well as MAdCAM-1 expression by dendritic cells (DC). Studies of effector immune responses in L-selectin-deficient (L-Sel^{-/-}) mice revealed that Ab responses in NP and RT, but not intestinal lamina propria (iLP) were abated 16 days post-i.n. CT immunization. Investigation of lymphocyte homing receptors revealed that an L-selectin^{low}/ $\beta 7^{\text{low}}$ ($\alpha_4\beta_7^+$) B lymphocyte population provides effector immunity in NP and RT, while iLP effector immune response is contained within the L-selectin^{low}/ $\beta 7^{\text{low}}$ ($\alpha_4\beta_7^+$) B lymphocyte subpopulation as well as a unique L-selectin^{low}/ $\beta 7^{\text{high}}$ (α_E^+) B lymphocyte population that is unaffected by the loss of L-selectin. Moreover, oral immunization of L-Sel^{-/-} mice induced response in all effector sites, and increased response in CONALT suggesting a definite difference in the effect of loss of L-selectin on inductive immune responses in PP. Finally, long-term immunization studies revealed that effector immune responses in L-Sel^{-/-} NP and RT are delayed, not eliminated, and Ab response was significantly increased in L-Sel^{-/-} CONALT. Together, these results highlight the important of L-selectin-PNAd homing interactions in induction of immunity after i.n. immunization, and support the concept of the compartmentalization of the CMIS.

CHAPTER 1

LYMPHOCYTE HOMING AND THE COMMON MUCOSAL IMMUNE SYSTEM

Mucosal ImmunologyThe common mucosal immune system

The ability of immunization at one mucosal site to effect protective immune responses at all mucosal surfaces was first suggested in the 1890's. Paul Erlich demonstrated that feeding increasing doses of ricin to rodents not only prevented killing after subcutaneous administration of the toxin (oral tolerance), but also prevented toxicity in the eye (reviewed in 1). In much later studies it was learned that secretory IgA (S-IgA) (reviewed in 2) antibodies specific to the mucosal surfaces, such as the intestine, nasal passages, salivary glands, and mammary glands, are protective against pathogens (3-8). Anatomical studies of lymphoid tissue in the gut revealed that the unique lymphatic nodule, the Peyer's patch (PP), first identified by Johannes Conrad Peyer in 1673, is where lymphocytes first encounter antigen (9). Subsequent intestinal immunity depends upon lymphocyte activation in these structures, collectively referred to as the gut-associated lymphoid tissue (GALT), and eventual homing to intestinal effector sites (10). Likewise, anatomical studies revealed similar lymphoid structures in the bronchi (bronchus-associated lymphoid tissue, or BALT) (11, 12) and a similarity to the architecture of the PP in the structures of the tonsils and adenoids. Such similarities in mucosal structure and antibody secretion led to characterization of the mucosal surfaces

as part of a greater "common mucosal immune system" (CMIS) (13). Through the 1970's, many experiments revealed that oral immunization induced antigen-specific IgA responses at mucosal surfaces throughout the body, from salivary and ocular secretions (14, 15), to mammary secretions (16), to reproductive tract (RT) immunity (17, 18). Such observations have led to the speculation that "...the mucosal immune system may be more generalized even than originally thought" (1).

Compartmentalization of the common mucosal immune system

More recent studies have revealed that the CMIS may, in fact, be compartmentalized. Oral vaccination in humans induces a robust intestinal response and a response in the RT, but little to no response in the upper respiratory tract (19). In contrast, intranasal (i.n) vaccination induces the expected strong IgA antibody (Ab) response in the nasal passages (NP) and upper respiratory tract and systemic IgG responses (20-30). I.n. immunization induces elevated CTL responses to viral and ovalbumin peptides as well (31-33). I.n. immunization also induces IgA response in the intestine, and most importantly, Ab production in the RT (19, 27, 30, 34-42). Throughout the past decade, many investigators have focused on i.n. immunization as a potent method for inducing RT immunity for several reasons. First, i.n. immunization provides a noninvasive route of administration of antigen, particularly advantageous when booster doses are required. Moreover direct vaginal immunization can be affected by hormonal influences and epithelial cell turnover during the estrous cycle (43). Finally, direct vaginal immunization does not stimulate immunity at other mucosal surfaces and

produces variable systemic Ab responses (39, 41). Successful protection in murine RT has been achieved using i.n. immunization with bacterial proteins (39, 40, 44), viral proteins and peptides (27, 34, 45), attenuated virus (41), recombinant viral vectors (32, 36, 37), and plasmid DNA (42, 46). In addition, studies in horses, non-human primates, and humans also show that i.n. immunization is a viable route for inducing upper and lower respiratory tract as well as reproductive tract immunity in various species (19, 30, 47-49). I.n. immunization shows promise as an effective means to stimulate local respiratory immunity and induce protective immunity in the RT. Thus, it is important to determine the mechanisms by which lymphocytes traffic from inductive sites in the NP to distal mucosal sites.

The mucosal immune system consists of inductive and effector sites

In order to effectively induce immunity throughout mucosal surfaces, antigen must first be processed in the organized lymphoid structures of the mucosal inductive sites. Lymphocytes are activated and assume memory phenotypes in these sites, and then disseminate to the lamina propria of the mucosal effector sites. The hallmark of effector site immunity is the production of S-IgA, though CD4⁺ and CD8⁺ lymphocytes also contribute to protection at these sites (50).

Antigen is first encountered and processed, and initial activation and expansion of B and T cells takes place in mucosal inductive sites. The intestinal Peyer's patch (PP) is the most widely characterized inductive site. While the PP shares morphology with other lymphoid sites, such as the PLN, it is highly specialized to induce mucosal immunity. B

cell follicles, and T cell areas are contained within the PP. The PP also contain a specialized lymph epithelium known as the sub epithelial "dome" area (SED; Figure 1). At the top of this dome lie specialized epithelial cells, known as "M" cells (51, 52). These cells take up antigens from the intestinal lamina propria, in effect "sampling" the contents of the intestine for antigens and microorganisms (52-56). "M" cells transport antigen to the underlying region of the SED which contains a high concentration of dendritic cells (DC) with a smaller population of macrophages. It is thought that immature DC ($CD11c^+$, NLDC-145⁻) take up and process antigen in the SED and then migrate to the T cell regions of the PP, where they assume a more mature phenotype ($CD11c^+$, NLDC-145⁺) and present antigen to the T cells (57). Subsequent activation of $CD4^+$ T cells provides the necessary T helper (Th) functions for the activation of and differentiation of B lymphocytes. The majority (60-70%) of B lymphocytes in the germinal centers of the PP are surface IgA (sIgA)⁺ and are considered to be precursors of IgA plasma cells (58, 59). These lymphocytes then drain from the Peyer's patch, into the mesenteric lymph node, and to the thoracic duct (60). Activated lymphocytes then enter the bloodstream, where they eventually migrate to the lamina propria of mucosal effector sites, and differentiate into IgA plasma cells. The migration of activated lymphocytes to specific effector sites has yet to be completely understood; however, it is likely that specific addressin-homing receptor interactions facilitate the trafficking of lymphocytes to the effector sites.

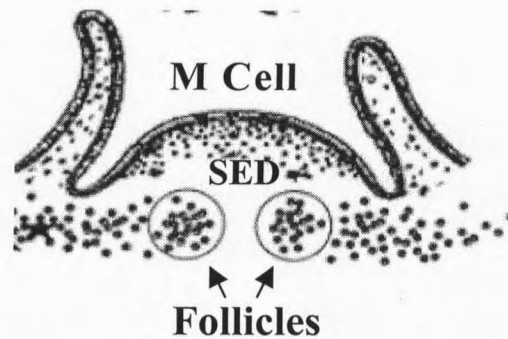


Figure 1. Structure of the Peyer's patch, the mucosal inductive site for the intestine. The epithelial cell layer containing M cells, the underlying subepithelial dome (SED) region, and B cell follicles are depicted

Effector sites of the mucosal immune system are defined as sites protected by mucus secretions. These sites include the nasal lamina propria (LP), intestinal LP, oral cavity, and the reproductive tract. Activated B cells migrate from inductive sites to the LP of the effector sites, where they mature into IgA plasma cells. Polymeric IgA produced by the plasma cells in the LP compartment binds to the polymeric immunoglobulin receptor (pIgR) expressed on the basolateral surface of the overlying epithelial cells. This binding interaction triggers transcytosis of the IgA-pIgR receptor complex to the apical surface of the epithelial cells, and the pIgR receptor is cleaved enzymatically. The released polymeric IgA retains a fragment of the pIgR referred to as secretory component (SC), which is thought to protect the newly synthesized secretory IgA (S-IgA) from proteolytic cleavage. (61-63). While small amounts of IgG and IgM secreting plasma cells (10-30% combined) are also found in the mucosal effector sites, particularly in the human reproductive tract (64-66), the majority of immunoglobulin produced is S-IgA (50).

Th and cytotoxic T cells (CTLs) also play key roles in the LP. Depending on the type of antigen administered during immunization, CD4⁺ Th cells secrete cytokines to drive a Th1- or a Th2-type response. Intracellular pathogens, such as *Salmonella* induce a Th1 type response, characterized by the secretion of IFN- γ , IL-2, and the induction of cell-mediated immunity. Extracellular pathogens, such as enterotoxigenic *E. coli* (ETEC), or mucosal adjuvants such as cholera toxin (CT), induce a Th2-type response, characterized by IL-4, IL-5, IL-6, and IL-10 production. Th2-type cytokines are more efficient in promoting B cell responses and preferentially stimulate IgG1, IgE, and IgA in the mouse (Reviewed in 67). Although Th2-type responses seem to predominate in mucosal sites, the type of pathogen that induces an immune response can also impact the type of Th cell response produced.

NALT is an inductive site for the nasal passages

A unique nasal-associated lymphoid tissue (NALT) has been identified in rodents (68-70) and birds (71) that represents the oropharyngeal lymphoid tissues of the upper respiratory airways. This structure is believed to be analogous to human Waldeyer's ring (tonsils and adenoids) (72), and consists of bilateral lymphoid structures dorsal to the cartilaginous soft palate. It is thought, much like the PP, to behave as a mucosal inductive site. This resemblance is evident in both the organization and structure of NALT as well as its cellular composition. First, there is an epithelial layer overlaying the NALT which contains "M" cells and an SED region thought to mediate antigen entry, uptake, and presentation much like that observed in the PP (68, 69, 73, 74). In addition,

there is a unique organization of both B cell zones and T cell areas similar to the structure of the PP, though the percentage of B220⁺ cells (55%), CD4⁺ cells (32%), and CD8⁺ cells (9%) in NALT more closely resembles that of the spleen than the PP, which contains nearly 70-80% B cells. (26, 75, 76). Given its proximity to the nasal LP, and its similarity in structure to the gut-associated lymphoid inductive tissue, the PP, NALT is assumed to significantly contribute to the stimulation of mucosal effector precursors for the upper airways.

Studies of NALT response after i.n. immunization have provided insight into the unique role of this putative nasal inductive site. After i.n. immunization with cholera toxin (CT) antibody-forming cells (AFC) were present in NALT, whereas oral immunization induced only CT-specific IgA cells in the PP (26). In addition, both IgA and IgG responses were observed in NALT 7 days post influenza immunization in mice (77), and AFC of all isotypes have been observed as rapidly as three days following i.n. immunization with bacterial proteins (78, 79). I.n. immunization with influenza virus stimulates Ag-specific IgA, IgG, and IgM AFC response in NALT by day 8 post-infection, and these Ab responses are maintained as long as five months post-infection (80). In addition, both Th and CTL responses, as well as long term memory proliferation are induced in NALT subsequent to i.n. immunization with various antigens (79, 81-83). While these studies show that NALT likely plays an important role in the induction of mucosal immunity following nasal immunization, responses to antigen also occur in the lymph nodes (LN) that drain the NALT.

Role of CONALT in the induction of nasal immunity

Several LN have been identified that drain the NP, brain, and the skin of the head and neck. We refer to these tissues collectively as the cranial, oral, and nasal-associated lymphoid tissues, or CONALT (84). The CONALT encompasses the facial or parotid gland LN (PRLN) located posterior to the parotid gland, the submaxillary gland LN (SMLN), and the deep cervical LN (CLN) located dorsal to the brachial plexus deep within the musculature of the neck (60). Studies of drainage patterns revealed that the SMLN drain NALT, nasal passages and tongue area, while the PRLN drain the skin of the head and neck region as well as the conjunctiva (78, 85). The deep CLN drain the NALT, SMLN, PRLN, and, in the case of antigen overload, the NP directly (60, 86, 87). CLN have also been shown to contain antigens draining from the brain (88-90), suggesting that the deep CLN play a role as a central node of the head and neck. Lymphocytes that collect in CLN drain via the cervical duct and then re-enter circulation via the subclavian vein (60). The relationship between antigen drainage in the NALT and CONALT has been further elucidated by microsphere immunization experiments, where it was determined that i.n. administered fluorescent microspheres first appeared in NALT 15 minutes post immunization, in SMLN at 24 hours post immunization, and in the CLN as late as 10 days post-immunization (91). IL-4 and IFN- γ secretion in response to i.n. microparticle injection appears first in NALT, then in the CLN and SMLN a week later (83). In addition, activated lymphocytes draining from the NALT pass through the SMLN and CLN as they are disseminated throughout the immune system.

It has been suggested that CONALT and NALT response to antigen must be

stimulated in order to effect intranasal immunity. I.n. administration of bacterial protein induces IgG and IgA AFC in SMLN and CLN, and also stimulates antigen-specific proliferation mainly in the CLN that begins two days after immunization and remains as late as six months post-immunization (78). More importantly, similar responses were observed after oral immunization with the same antigen but only in the presence of cholera toxin B subunit (CT-B) adjuvant. These data indicate that antigen-specific responses formed directly as a result of i.n., but not intragastric route of immunization in these LN. Also, IgA response following nasal immunizations with T cell dependant antigens appears restricted to the NALT and CLN (86). In addition, CLN have been shown to produce strong CTL responses after i.n. HIV peptide immunization (33). Finally, after nasal infection with influenza virus, there is greater accumulation and recovery of virus-specific CD8⁺ cells in the SMLN than in NALT, leading to speculation that cell-mediated immunity to influenza virus infection might be induced in the SMLN, rather than in the NALT (81).

CONALT also play a role in the induction of immune responses at sites other than the NP. While oral immunization induces specific salivary Abs, i.n. immunization appears to be more efficient at stimulating sustained, elevated salivary immune responses (92). This effect is also evident in the CONALT where i.n. and to a lesser extent, oral immunization, with bacterial protein antigens coupled to CT-B produces strong IgA and IgG responses in the SMLN and CLN, resulting in immune S-IgA Abs in saliva (78). However, IgG responses in the PRLN are more effectively stimulated by subcutaneous (s.c.) rather than i.n. immunization. CLN have been proven to be important in the

triggering of allergic responses to particulate antigens (93) and have been shown to play an important role in the induction of immunity in the central nervous system, as removal of the CLN ablates experimental autoimmune encephalomyelitis (94).

Though it is clear that immune responses to i.n. introduced antigen first begin in NALT and CONALT, it is unknown by what mechanisms mucosal immunity is induced at distal mucosal effector sites, and if lymphocyte trafficking from the nasal inductive sites follows unique and specific patterns.

Lymphocyte Homing

Lymphocytes display specific trafficking patterns

Since 1964, it has been known that lymphocytes are capable of continuously trafficking from the blood to the lymph and back again (95). More importantly, these studies showed that naive lymphocytes migrate according to their site of origin, that is, mucosally derived lymphocytes return to the intestine and PP, while peripherally derived lymphocytes return to peripheral LN (PLN) (96). Memory lymphocytes also possess the ability to return to the site of initial encounter of antigen (97). More importantly, memory lymphocytes display mucosal vs. peripheral routes of recirculation as cutaneous immunization induced subsets of T and B lymphocytes that trafficked to the skin while lymphocytes activated in the GALT preferentially returned to iLP, PP, and mesenteric LN (MLN) (97-100). Lymphocytes that preferentially trafficked to gut expressed primarily IgA, while lymphocytes that returned to peripheral sites were more likely to express IgG. Interestingly, such studies also provided early evidence for the

compartmentalization of CMIS, as lymphocytes derived from BALT preferentially migrated to the lung rather than intestine, and expressed IgG rather than IgA (17). Clearly, specialized cell-to-cell interactions exist that control tissue-specific homing and provide for mucosal vs. peripheral lymphocyte trafficking.

The multistep model of lymphocyte homing

Lymphocyte homing to LN is controlled via a complex series of interactions between specialized vascular endothelium and adhesion receptors on microvilli of circulating lymphocytes (101, 102). The adhesion receptors, known as lymphocyte homing receptors, consist of selectins and integrins, which interact with specialized addressin ligands expressed by high endothelial venules (HEV) (103, 104), or adhesion molecules up-regulated as a result of inflammatory signals in the flat-walled endothelium of the extralymphoid sites, such as gut (105, 106). Selectins initiate the initial rolling and reversible tethering interaction and allow for lymphocyte "sampling" of the local microenvironment. If the required chemoattractants are present (107, 108), integrins present on the lymphocyte surface are activated through G-protein linked receptor signaling, leading to the firm arrest of the lymphocyte to the endothelium (109). Additional chemokine signals are then required to complete the final step of lymphocyte homing: transendothelial migration (110). All of the steps of lymphocyte homing up to transendothelial migration are reversible if the right chemical signals are not present, leading to an exquisitely controlled system that can regulate the recruitment of specific lymphocyte subsets into different tissues.

Addressin expression is tissue specific

A member of the immunoglobulin superfamily has been identified as the addressin that mediates initial lymphocyte binding to PP HEV. This mucosal cell adhesion molecule-1 (MAdCAM-1) binds to the integrin $\alpha_4\beta_7$, and L-selectin on naive lymphocytes, and can mediate both the initial tethering and tight binding interactions in the three-step model of lymphocyte homing (101, 111). While MAdCAM-1 is expressed at high levels on the HEV of the PP and the MLN, as well as flat-walled endothelium in the intestinal LP (106, 112), and vessels in the marginal sinus of spleen (113, 114), it is present at very low levels or not at all on the HEV of PLN (115).

In contrast, the predominant addressin expressed in PLN is peripheral node addressin (PNAd). PNAd is defined as several carbohydrate epitopes recognized by the MECA 79 antibody. These carbohydrate moieties decorate different glycoprotein backbones on the HEV (116), and all must be sulfated for recognition by the PNAd ligand, L-selectin (117, 118). MECA 79 binds to a specific carbohydrate expressed by the MAdCAM-1 glycoprotein backbone (119) as well as to carbohydrate expressed by soluble glycosylation-dependent cell adhesion molecule (GlyCAM)-1 (120), cell associated CD34 (121), and soluble and cell associated sulfated glycoprotein (Sgp) 200 (118). L-selectin-PNAd interactions mediate almost all naive lymphocyte binding to PLN HEV (122, 123), as well as some binding in the MLN (106). L-selectin-PNAd interactions also contribute to binding of naive lymphocytes to the PP through the expression of PNAd carbohydrate on the MAdCAM-1 glycoprotein backbone (101, 119). High levels of PNAd are also expressed on the HEV of human tonsil (124). Therefore,

while L-selectin-PNAd interactions are thought to mediate the majority of naive lymphocyte homing to PLN, there appears to be a role for these interactions in mucosal tissues as well. It is currently unknown if the NALT behaves like the human tonsil and expresses PNAd, though preliminary homing results suggest that this tissue may indeed express a more "peripheral" addressin phenotype (125).

Lymphocyte homing receptors

Addressin ligands that mediate binding to endothelium consist of selectins and integrins. The extracellular protein domains of the selectins contain an NH₂ terminal lectin domain, which binds sialyl Lewis-X carbohydrates, followed a single epidermal growth factor (EGF) - like repeat, and a varying number of repeating short consensus sequences followed by a transmembrane domain anchored by a short cytoplasmic tail. (126, 127). The ligand for PNAd, L-selectin, is expressed on all naive lymphocytes and mediates the initial rolling interaction in the multistep model of lymphocyte homing (102, 128). In fact, binding via L-selectin interaction requires a threshold hydrodynamic shear (129), which contributes to the regulation of the function of L-selectin on lymphocytes as they traffic through the bloodstream.

Integrins can also mediate the initial, as well as the secondary, steps of lymphocyte homing. Integrins are heterodimers that consist of noncovalently associated α and β subunits. To date, fourteen different α subunits and eight different β subunits, which can combine to form twenty different heterodimers have been identified. The larger α subunits, which determine the specificity of the integrin binding, have large

extracellular binding domains consisting of three to four cation binding domains, a transmembrane region, and short cytoplasmic tails. The smaller β subunits contain extracellular domains consisting of cysteine residues clustered in four repeated motifs followed by a transmembrane domain and also have short cytoplasmic tails (reviewed in (130)). The $\alpha_4\beta_7$ heterodimer, expressed at low levels on nearly all naive lymphocytes, can participate in both rolling and adhesion to the HEV of PP (101), and may act to slow selectin-initiated rolling (mediated via PNA_d expression on MAdCAM-1) in order to allow for tight adhesion of lymphocytes. However, in the case of the $\alpha_4\beta_7$ heterodimer interaction with MAdCAM-1 expressed in the iLP, the integrin provides both rolling and tight adhesion interactions (102).

$\alpha_E\beta_7$ is an intestine-specific integrin

Unlike other integrins, the $\alpha_E\beta_7$ integrin is present mainly on some CD4⁺ and most CD8⁺ T lymphocytes located within the iLP and intestinal epithelial lymphocyte (IEL) compartments of mouse and human (131-133). This integrin has also been observed on CD8⁺ thymocytes and is expressed at higher levels on CD4⁺ and CD8⁺ PP and MLN lymphocytes than those in spleen or PLN (134). No expression of $\alpha_E\beta_7$ integrin has been observed on B lymphocytes. Unlike $\alpha_4\beta_7$, $\alpha_E\beta_7$ is not capable of binding to MAdCAM-1 nor does it appear to play a role in lymphocyte homing to the intestine (135). Instead, $\alpha_E\beta_7$ appears to be induced and maintained primarily by the secretion of TGF- β 1 by epithelial cells, and binds to epithelial cadherin (E-cadherin) expressed on the basolateral surface of epithelial cells (136-139). It is believed that $\alpha_E\beta_7$ contributes to the retention

of lymphocytes, particularly in the IEL compartment, since α_4 deficient mice (lacking $\alpha_4\beta_7$) have normal IEL development (140), while β_7 deficient mice (lacking both $\alpha_4\beta_7$ and $\alpha_E\beta_7$) show reduced numbers of IEL (141). However, recent studies of antiviral CD8⁺ cell homing have shown that $\alpha_E\beta_7$ is not required for trafficking or long term retention in the IEL (142). Still more studies have shown that loss of α_E does indeed reduce the number of T cells found in iLP, and that $\alpha_E\beta_7$ can bind to a non-E-cadherin ligand expressed on human endothelial cells (143, 144). Together, these results suggest that while $\alpha_E\beta_7$ may not play a role in selective CD8⁺ lymphocyte trafficking to iLP and IEL, this integrin may contribute to formation of the IEL and possibly to extravasation into the iLP. More importantly, $\alpha_E\beta_7$ may also represent an intestinal-specific integrin that is not present in the non-intestinal mucosal effector sites.

Expression of addressins by follicular dendritic cells may contribute to lymphocyte recruitment and retention

Recent evidence suggests that stromal elements, most likely follicular dendritic cells (FDC), may express addressins (145). While the function of this addressin expressed on the FDC is unknown, it has been suggested that stromal MAdCAM-1 and vascular cell adhesion molecule-1 (VCAM-1) play a role in lymphocyte retention within the follicle. Szabo *et al* (145) showed that both MAdCAM-1 and VCAM-1 in the follicles of PP and PLN bound lymphocytes expressing their respective ligands, $\alpha_4\beta_7$ and $\alpha_4\beta_1$. In addition, it has been reported that binding to VCAM-1 plays a role in B cell selection, as lymphocytes bound to VCAM-1 showed resistance to apoptosis (146). These results

suggest that addressins expressed in the follicles of lymphoid sites play an important role in the retention of antigen-specific T and B cells.

This evidence also suggests that the division of addressins into “mucosal” and “peripheral” types holds true for FDC-expressed MAdCAM-1 and VCAM-1. Szabo *et al* (145) found that FDC in the PP expressed MAdCAM-1, while FDC in the PLN expressed VCAM-1. More importantly, the tonsil, which is considered analogous to NALT, expresses VCAM-1 but not MAdCAM-1 within its follicles (147). This suggests that NALT might express a more “peripheral” phenotype of follicular addressins and supports our contention that addressin expression varies between mucosal tissues.

Different homing receptor-addressin pairs mediate memory lymphocyte homing to peripheral and mucosal sites

Immune responses that induce memory result in upregulation of specific homing receptors on lymphocytes and addressins that mediate binding in the HEV of LN. In particular, MAdCAM-1 is expressed in normal and inflamed intestine of humans and mice, in both the PP and LP, as well as in inflamed mucosal sites (148). Lymphocytes that home preferentially to these sites express high levels of $\alpha_4\beta_7$ (149, 150). Only $\alpha_4\beta_7^{\text{high}}$ B lymphocytes produced protective antibody against rotavirus infection (151). In contrast, lymphocyte homing to non-gut mucosal sites, such as the upper airways in humans and sheep, does not appear to be mediated by MAdCAM-1 - $\alpha_4\beta_7$ interactions (152-154). Since the NALT acts as an inductive site for the respiratory tract, which contains both mucosal (upper airways and bronchi) and systemic (alveolar spaces), it seems likely that memory lymphocytes induced in the NALT may not be dependent upon

$\alpha_4\beta_7$ -MAdCAM-1 interactions for homing.

The roles of L-selectin and $\alpha_4\beta_7$ have been further defined by the creation of L-selectin deficient (L-Sel^{-/-}) (155, 156) and β_7 deficient (141) mice. L-Sel^{-/-} mice show a marked reduction in cellularity in PLN, while the size of PP, where homing of lymphocytes is compensated by $\alpha_4\beta_7$ - MAdCAM-1 interactions, are not affected (155). Loss of L-selectin illustrates the role this homing receptor plays in the migration of memory lymphocytes to peripheral sites of inflammation, as L-Sel^{-/-} mice show reduced peripheral delayed-type hypersensitivity responses and delayed skin graft rejection (157-159). In contrast, β_7 - deficient mice, which lack both $\alpha_4\beta_7$ and $\alpha_E\beta_7$, show a drastically impaired formation of GALT but not PLN, highlighting the importance of β_7 integrin in lymphocyte homing to the intestinal, but not the peripheral tissues (141). Interestingly, studies of β_7 /L-selectin double deficient mice revealed that lymphocyte homing to MLN, which expresses both MAdCAM-1 and PNA_d is mediated by both L-selectin and $\alpha_4\beta_7$ (160). These studies underscore the important differences between L-selectin and $\alpha_4\beta_7$ in the formation of peripheral and mucosal sites and the role of L-selectin in peripheral immune responses. However, no studies have yet examined the effect of loss of L-selectin on mucosal effector sites.

Roles of L-selectin and $\alpha_4\beta_7$ in memory B lymphocyte homing

Though studies in mice and humans indicate that $\alpha_4\beta_7$ expression is necessary for the induction of mucosal immunity to rotavirus (149, 151, 161), new evidence suggests that the mediation of lymphocyte homing to various effector sites may be controlled or

compensated for by other lymphocyte homing receptors. β_7 -deficient mice still mount effective immune responses to rotavirus, and Ag-specific CD8⁺ lymphocytes remain capable of trafficking to the intestine in these mice (142, 162). Much less is known about the trafficking of B cells in β_7 -deficient mice, though IgA response in rotavirus infected β_7 -deficient intestine was decreased.

Immediately following activation, B lymphocytes shed L-selectin, whereas memory B lymphocytes up-regulate L-selectin after secondary immunization, allowing for the re-entry of memory B lymphocytes into the circulation (163). Decrease or loss of L-selectin expression on B lymphocytes limits their ability to traffic to LN and suggesting that humoral responses in L-Sel^{-/-} mice must be abated as well (164, 165). However, IgM and IgG1 responses following intraperitoneal (i.p.) immunization were actually increased in L-Sel^{-/-} mice. Responses immediately following s.c. immunization were delayed but secondary immune responses in L-Sel^{-/-} mice were greater than those in their L-Sel^{+/+} counterparts. These results indicate that B cell responses might not be dependent upon L-selectin mediated trafficking; however, the role of L-selectin in generation of memory humoral responses in humans has yet to be defined. Immunohistochemical staining of PP B lymphocytes revealed that the majority of naive (sIgD⁺ CD19⁺ CD20⁺ CD45RA⁺) B lymphocytes were weakly positive or negative for $\alpha_4\beta_7$ and expressed some L-selectin, though samples were variable. Memory B lymphocytes showed more intense $\alpha_4\beta_7$ staining and very few of these cells expressed L-selectin (166). Other studies of normal human lymphoid tissue revealed the presence of L-selectin on mantle zone B lymphocytes, but not on memory lymphocytes at the site of

inflammation (167). However, identification of AFC after oral, rectal, and parenteral administration of *Salmonella typhi* revealed that Ag-specific AFC in the blood showed both $\alpha_4\beta_7$ and L-selectin expression, though expression levels of these homing receptors varied depending on the route of immunization (168, 169). These results suggest that L-selectin, and $\alpha_4\beta_7$ play a role in the induction of memory B cell responses in both rodents and humans.

Statement of the Hypothesis

NALT has been identified as a unique mucosal inductive site that stimulates responses in the NP and upper airways, and in the reproductive tract. Given the remarkable ability of i.n. immunization, but not oral immunization to preferentially induce immunity in the RT it is likely that there exists a compartmentalization of the CMIS. The ability of NALT to induce immunity at local sites such as the NP and the RT may be related to the homing receptor-addressin interactions that allow for lymphocyte trafficking to and from this site. Whereas lymphocyte homing receptor-addressin interactions that mediate lymphocyte trafficking to the GALT have been well defined, it is unknown what homing receptors mediate lymphocyte trafficking to NALT. Evidence does indicate that trafficking to and from the NP and RT is not mediated by intestinal $\alpha_4\beta_7$ - MAdCAM-1 interactions. Therefore, I hypothesize that lymphocyte trafficking interactions to and from the NALT are mediated via PNAd-L-selectin interactions. Furthermore, L-selectin plays an important role in the induction of immunity in the non-intestinal mucosal effector sites.

In Chapter 3 of the text I describe the identification of the addressins expressed by

the HEV of naive NALT, the homing receptors expressed by the lymphocytes of this tissue, and determine the functionality of the expressed addressins and homing receptors in lymphocyte binding to NALT. The same studies were performed on the related draining CONALT and these results are discussed in Chapter 4, further elucidating the role of peripheral addressin-homing receptor interactions in the inductive tissues of the head and neck. In Chapter 5, I describe the changes that occur in lymphocyte homing to NALT following immunization with a potent mucosal adjuvant, cholera toxin (CT). The role of L-selectin in the induction of immunity in the distal effector sites after both i.n. and oral immunization was determined in and is described in Chapters 6 and 7. An unexpected effect of loss of L-selectin in inductive tissue and long term effector immune response after i.n. immunization is detailed in Chapter 8.

Together, these results support my hypothesis that lymphocyte homing to and from the inductive sites of the head and neck is mediated via peripheral addressin – homing receptor interactions and suggests that the CMIS may be compartmentalized into “intestinal” and “non-intestinal” mucosal effector sites.

CHAPTER 2

MATERIALS AND METHODS

Mice

Specific pathogen-free BALB/c or C57BL/6N mice were purchased from the National Cancer Institute at 5-6 wk of age and maintained in the Animal Resources Center at Montana State University (Bozeman, MT). Breeding pairs of C57BL/6-TgN(ACTbEGFP)10sb mice (C57BL/6-GFP; (170)) and L-Sel^{-/-} mice on a B6 background (155, 156) were purchased from The Jackson Laboratories (Bar Harbor, ME), and colonies were established and maintained in the Animal Resources Center at Montana State University. All mice were kept under pathogen-free conditions in horizontal laminar flow cabinets and were fed sterile food and water *ad libitum*. The mice were free of bacterial and viral pathogens as determined by Ab screening and by histopathologic analysis of major organs and tissues. The mice used in these experiments were between 5-8 wk of age.

Immunizations

Mice were immunized via intranasal drip on day 0 with 5 µg CT in 10 µl sterile PBS (List Biological Laboratories, Campbell, CA), and boosted on days 7 and 14 post-primary immunization with 2.5 µg CT. For oral administration of CT, mice were orally

gavaged with 200 μ l of 50%-saturated sodium bicarbonate solution, followed by 10 μ g CT/200 μ l sterile PBS using a #22 oral gavage needle. Mice were orally boosted with 10 μ g CT at days 7 and 14 post-primary immunization.

Collection of serum, fecal, and vaginal samples

Blood was collected from mice through saphenous vein bleeding. Fresh fecal pellets were collected from individual mice. Pellets were treated with 10X volume/weight of 50 μ g/ml soybean trypsin inhibitor (Sigma, St. Louis, MO) and vortexed for 30 minutes at 4°C. Vaginal secretions were collected by gently pipetting 75 μ l of sterile PBS in and out of the vaginal vault. All samples were placed in microcentrifuge tubes and held on ice until centrifugation. Samples were centrifuged in an Eppendorf 5415 C microcentrifuge (Brinkman Instruments Inc. Westbury, NY) for 30 minutes at 13,000 rpm at 4°C for 30 minutes, and supernatants containing secreted Ab were collected and stored frozen until use.

Anti-CT-B ELISA

Falcon® Micro-test III™ Flexible assay microtiter plates (Becton-Dickinson, Oxnard, CA) were coated with 50 μ l/well of 5 μ g/ml CT-B (List Biological Labs) in sterile PBS and incubated overnight at room temperature. The plates were blocked with 200 μ l/well PBS + 1.0% BSA for 1 hour at 37°C. Plates were washed three times with PBS and twice with PBS-Tween-20®, and serum dilutions in ELISA buffer (PBS + 0.5% BSA + 0.05% Tween-20®) were added at 50 μ l/well, and plates incubated at 4°C overnight.

Plates were washed, and 50 μ l/well of detecting goat anti- mouse IgG or IgA-horseradish peroxidase (HRP) conjugate (1 μ g/ml; Southern Biotechnology Associates) was added and the plates were incubated at 37°C for 1.5 hours. HRP was visualized by the addition of 50 μ l/well of ABTS substrate (Moss Inc.). Optical density was determined by reading the plates at 415 nm, and endpoint titers were expressed as the reciprocal of the last sample dilution giving an absorbance > 0.1 over the value of negative control wells after a 1 hour incubation.

Tissue isolation and collection

MLN, PLN, PP, PRLN, SMLN, and CLN were isolated from normal BALB/c and C57BL/6N mice. Each set of lymphoid tissue was pooled from five mice, washed in RPMI-1640 medium (BioWhittaker, Walkersville, MD), and frozen using Tissue Tek[®] O.C.T. compound embedding medium (Miles Inc., Elkhart, IN) in a 15 mm by 15 mm Tissue Tek[®] Cryomold. Samples were stored at -80°C until use. For double immunofluorescent and immunoperoxidase staining, frozen sections were cut at a thickness of 5 μ m, air-dried, fixed in acetone at 4°C, and air-dried again before rehydration.

NALT tissues were collected by removing the soft palates as previously described (76, 83). Briefly, euthanized mice were decapitated, their heads immobilized, and the lower jaws, including tongue, were removed. Palates were scored along the outer edge and gently removed. Palates were then washed in RPMI 1640 medium, blotted dry, and arranged in cryomolds with their ventral faces (containing NALT) oriented at the bottom of the mold and frozen in O.C.T. as described above.

For flow cytometry and ELISPOT analysis, LN were removed and subjected to Dounce homogenization. The resulting cell suspensions were filtered through Nitex fabric (Fairview Fabrics, Hercules, CA), washed with RPMI 1640 medium and centrifuged at in a Beckman GPR tabletop centrifuge (Beckman Instruments Inc. Palo Alto, CA) for 1500 rpm for 5 minutes. The resulting cell pellet was resuspended in FACS buffer (Dulbecco's phosphate buffered saline [dPBS]; + 2% Fetal Bovine Serum; Hyclone), or complete medium (CM; RPMI 1640 + 10% FBS + 10 mM HEPES Buffer + 10 mM non-essential amino acids + 10 mM sodium pyruvate + 10 units/mL penicillin/streptomycin).

NALT lymphocytes were isolated for flow cytometry by Dounce homogenization as described for lymph node cells. For ELISPOT cell isolation, the soft palate was removed from the head of the mouse and placed in a 200U/ml 200 U/ml collagenase type IV solution (Sigma; (171)) in RPMI-1640 media containing .08U/ml DNase (Promega, Madison, WI) in a scintillation vial with a 2 cm magnetic stir bar. The palate was vigorously agitated on a magnetic stir plate for 45 minutes at 37°C, the resulting cell supernatant removed, filtered through Nitex, and cells were washed and resuspended in CM.

NP Lymphocyte Isolation

Mice were euthanized and NP removed from the head by scraping the turbinates from the nasal cavity, in a modification of a previous protocol (28) The nasal tissue was digested with 200 U/mL collagenase type IV solution containing 0.08 U/ml DNase in a glass 50 ml flask containing a magnetic stir bar. Following rapid agitation during

digestion at 37°C for 30 minutes, released NP lymphocytes were removed and fresh collagenase solution was added back to the flask. This procedure was repeated until digestion of the tissue was complete. Isolated cells were washed in complete medium and resuspended in a 40% Percoll® solution (Pharmacia, Uppsala, Sweden), and then layered over a 60% Percoll solution and subjected to gradient centrifugation. Lymphocytes were removed from the interface layer, washed, and resuspended in CM.

Intestinal LP lymphocyte isolation

A modification of a previous protocol was performed (172). Intestines were extracted from the mouse and the PP were carefully removed. Fecal material and mucous were flushed from the intestine using RPMI-1640 medium pushed through a #22 gavage needle. Intestines were then slid onto the needle and flayed open, minced into ~1mm pieces, shaken vigorously in CM to remove remaining mucous and fecal material, and the waste was filtered through a mesh screen. Intestinal tissues were then placed in RPMI 1640 medium containing 5% FBS (Hy-Clone) and 2 mM DTT (Sigma) in a 50 ml Teflon® flask containing a magnetic stir bar, and gently agitated on a stir plate at room temperature for 5 -10 minutes. This process results in the removal of the intestinal epithelial cell fraction. Supernatant was discarded, and DTT was rinsed from the intestinal pieces with RPMI-1640 medium. Intestinal tissues were returned to the Teflon flask, 50 U/ml collagenase type IV solution containing .08 U/ml DNase as previously described was added and the suspension was agitated at 37°C. After 10 minutes, the supernatant containing intestinal lamina propria cells was removed and washed, and fresh collagenase was added to the remaining intestine. The process was repeated 2 more

times, and lymphocytes isolated by Percoll gradient centrifugation as described above.

RT lymphocyte isolation

In a modification of a previous protocol (173), reproductive tracts, which include vagina, cervix, and uteri, were removed from mice, and the mucous and epithelium were flushed using RPMI 1640 medium. RT were then flayed open on a blunted 23 gauge needle, and minced into 1-2 mm pieces. These pieces were added to a 200 U/ml collagenase Type IV solution in a glass 50 ml flask containing a magnetic stir bar, and cells were released from the RT tissue by vigorous agitation on a magnetic stir plate at 37°C for 1 hour. Supernatant resulting from this process was removed and cells were washed in CM, and lymphocytes were isolated via Percoll gradient centrifugation as described above.

Double immunofluorescent staining for tissue addressins

Lymphoid tissue sections were incubated with MECA 367 mAb supernatant fluid (Table 1) or 10% normal rat serum for 30 minutes at room temperature (RT). Specific detection of MAdCAM-1 was obtained upon incubation of a 1:200 dilution of tetramethylrhodamine-5-(and-6-) isothiocyanate (TRITC) conjugated goat anti-rat IgG (H + L) Ab (Southern Biotechnology Associates, Birmingham, AL) in the dark for 30 min at RT. Sections were blocked with 1% rat serum for 15 minutes to bind any free arms of the goat anti-rat secondary Ab. Sections were then stained for PNAd using a 1:50 dilution of MECA 79 mAb (FITC; Table 1) in the dark for 30 minutes at RT. After rinsing, the slides were cover slipped using Immuno-Mount mounting media (Shandon-

Lipshaw, Pittsburgh, PA).

Immunohistochemical staining of MAdCAM-1 and VCAM-1

Serially cut frozen sections were rehydrated in dPBS containing 0.2% normal goat serum (NGS), and endogenous peroxidase was blocked with Dako peroxidase blocking reagent (Dako, Carpinteria, CA). Nonspecific binding was blocked by incubating the sections with 10% NGS in DPBS for 30 minutes at RT, followed by blocking for endogenous avidin and biotin with avidin/biotin blocking solution (Vector Laboratories, Burlingame, CA). Sections were incubated with 1:200 dilution of biotinylated rat anti-mouse vascular cell adhesion molecule-1 (VCAM-1) mAb (Table 1) or rat anti-mouse MECA 367 mAb supernatant fluid or with an isotype matched IgG control for 30 minutes at RT. Sections incubated with MECA 367 mAb were then treated with 1:250 dilution of biotinylated goat F(ab')₂ anti-rat IgG (γ and light chain, absorbed against mouse Ig; Biosource International, Camarillo, CA) for 30 minutes, and all sections were then incubated with a 1:500 dilution of streptavidin-HRP (SA-HRP; BioSource International). HRP was visualized by use of a 3-amino-9-ethyl-carbazole (AEC) staining kit (Vector Laboratories). After AEC development for 10 - 20 minutes, the sections were counterstained with hematoxylin (Richard-Allan Scientific, Kalamazoo, MI) and cover slipped using Immuno-Mount mounting medium.

Blocking of lymphocyte adhesion to HEV

A modification of the Stamper-Woodruff protocol was performed (174). Murine MLN were isolated and suspended in RPMI-1640 media and then subjected to Dounce

homogenization to release lymphocytes. The resulting cell suspension was filtered through NITEX fabric (Fairmont Fabrics, Hercules, CA). Following centrifugation, the MLN lymphocytes were resuspended in DMEM (Sigma, St. Louis, MO) containing 2.5% BSA at a concentration of 1×10^7 cells/ml.

Frozen tissue samples were cut to a thickness of 7 μm and allowed to air-dry for 30 minutes. A circle was drawn around each section with a hydrophobic pen. Sections were then placed on an orbital shaker (GeneMate, Intermountain Scientific Co., Bountiful, UT) at 4°C and 80 rpm. MECA 79 or MECA 367 mAb supernatant, or 5 $\mu\text{g/ml}$ solution of MVCAM.A mAb was added, and the Ab was rotated on the sections for 45-60 minutes to allow binding to MAdCAM-1, PNA_d, or VCAM-1, and then decanted. Lymphocytes (1×10^6) were added at a volume of 100 μl and rotated over the sections for 30 minutes to allow binding to HEV. Lymphocytes bound to HEV were fixed by placing sections in a cold 1.5% gluteraldehyde solution. To block lymphocyte binding via L-selectin, $\alpha_4\beta_7$, or $\alpha_4\beta_1$, cells were treated with 50 $\mu\text{g/ml}$ MEL-14 (rat anti-mouse L-selectin) mAb, FIB 30 (rat anti-mouse β_7) mAb, or 9EG7 (rat anti-mouse β_1) mAb respectively, for 30 minutes. Pretreated cells were then rotated over the sections as described above. Binding assays were analyzed by counting the number of cells bound/HEV in each LN and then comparing the average number of cells bound/HEV in the presence of Ab to the average number of cells bound/HEV in control sections.

Comparison of $\alpha_4\beta_7$ and L-selectin expression on lymphocytes

Lymphocytes were stained with either FITC-anti-B220, FITC-anti-CD4, or FITC-

anti-CD8 mAbs together with PE-MEL-14 rat anti-mouse L-selectin mAb, and biotinylated DATK 32 rat anti-mouse $\alpha_4\beta_7$ mAb for 30 minutes, washed, and then incubated with SA-CyChrome[®] (BD PharMingen) for 30 minutes. FL1, FL2, and FL3 parameters and compensation were set by the analysis of single-color FITC, PE, or CyChrome[®], respectively, while SA-CyChrome[®] conjugate was added to cells alone in order to determine a baseline fluorescence on the FL3 channel. Three-color analysis was performed using a FACSCalibur (Becton Dickinson, Mountain View, CA). Ten thousand events/sample were collected.

In vivo lymphocyte homing

Donor C57BL/6-GFP mice, whose nucleated cells constitutively express green fluorescent protein (GFP) (170) were euthanized, and SMLN, PRLN, and CLN were removed from 15-20 animals/experiment. Nodes were subjected to dounce homogenization, and lymphocytes were filtered through NITEX and combined. Lymphocytes were treated with 10 μ g of purified MEL-14, FIB-30, or with IgG2a isotype control in sterile PBS for 30 minutes at RT, and 12-15 x 10⁶ lymphocytes were then injected into recipient C57BL/6 mice via the tail vein with 100-250 μ g excess Ab. Recipient mice were sacrificed 4 hours or 24 hours post injection, and lymphocytes from NALT, CONALT, PLN, spleen, MLN, and PP were isolated. Percentage of GFP⁺ cells in lymphocyte suspensions was determined by FL-1 analysis on a FACSCaliber. Fifty thousand events/sample were collected.

Table 1. Monoclonal antibodies used in experiments

mAb	Isotype	Recognizes	Source
MECA 79	rat IgM	PNAd	(116)
MECA 367	rat IgG2a	MAdCAM-1	(106)
MEL 14	rat IgG2a	CD62L (L- selectin)	(123) BD PharMingen
FIB 30	rat IgG2a	β_7 integrin	(175)
FIB 504	rat IgG2a	β_7 integrin	(175), ATCC
MVCAM.A	rat IgG2a	CD106 (VCAM-1)	BD PharMingen
M290	hamster IgG	CD103 (α_E integrin)	BD PharMingen
9EG7	rat IgG2a	CD29 (β_1 integrin)	BD PharMingen
Ha2/5	hamster IgG	CD29 (β_1 integrin)	BD PharMingen
DATK 32	rat IgG2a	$\alpha_4\beta_7$ integrin (LPAM-1)	BD PharMingen
RA3-6B2	rat IgG2a	CD45R/B220	BD PharMingen
RM4-5	rat IgG2a	CD4	BD PharMingen
53-6.7	rat IgG2a	CD8 α	BD PharMingen
N418	hamster IgG	CD11c	ATCC
NLDC-145	rat IgG2a	DEC 205	ATCC

Flow cytometry and sorting of effector lymphocytes

NP, iLP, and RT lymphocytes combined from ten mice were stained for three or four color flow cytometry analysis as follows: cells were stained with anti- $\beta 7$ FIB 504 mAb supernatant fluid, followed by a biotinylated goat anti-rat IgG (BioSource, Camarillo, CA), then by addition of 1% rat serum, followed by streptavidin-APC. For three color analysis, anti-L-selectin mAb MEL-14-PE, and anti-B220-Cychrome mAb were used, while anti- $\alpha 4\beta 7$ heterodimer DATK-32-PE mAb, anti- αE M290-FITC mAb, and anti-B220-Cychrome mAb (see Table 1) were used for four color analysis. B220⁺ lymphocytes were sorted on a FACSVantage (BD-Biosciences) according to $\beta 7$ and L-selectin staining. $\beta 7^{\text{high}}$ and $\beta 7^{\text{low}}$ populations were sorted from L-selectin deficient (L-Sel.^{-/-}) and L-selectin positive C57BL/6 (L-Sel^{+/+}) iLP, while $\beta 7^{\text{low}}$ / L-selectin^{high} and $\beta 7^{\text{low}}$ L-selectin^{low} populations were sorted from L-Sel^{+/+} NP and RT. All cells were sorted at $\geq 97\%$ purity, counted, and the respective populations used in a B cell ELISPOT.

CT-B-specific ELISPOT

Mixed cellulose ester membrane-bottomed microtiter plates (Multi-Screen[®]-HA, Millipore Corp., Bedford, MA) were coated with 5 $\mu\text{g/ml}$ CT-B (List Biological Labs) in sterile PBS overnight at room temperature. The plates were blocked at 37°C for 2 hours with CM. A total of 100 μl of cells from each tissue at varying concentrations (2×10^6 - 1.25×10^5 lymphocytes/ml) were added to the wells, and the plates were incubated at 37°C overnight. Cells were removed, and the plates were washed three times with PBS +

0.1% Tween 20 and twice with PBS. For detection of mouse antibody, 100 μ l of 1 μ g/ml goat anti-mouse IgG and IgA-HRP conjugates (South. Biotech. Assoc.) were added to the wells, and the plates incubated overnight at 4°C. After washing as described above, the wells were developed with 100 μ l of AEC (Moss Inc., Pasadena, MD), and the reaction allowed to continue until spots developed (~ 30 minutes). The reaction was stopped with H₂O, the plates were allowed to dry overnight, and spot-forming cells were enumerated by counting under a low-power dissecting microscope (Leica Microscopy Systems LTD & Co. Heerbrugg, Switzerland).

Statistical analysis

Results were analyzed using a paired Student's *t* test. Significant *p* values are indicated.

CHAPTER 3

NASAL-ASSOCIATED LYMPHOID TISSUE: PHENOTYPIC AND FUNCTIONAL EVIDENCE FOR THE PRIMARY ROLE OF PERIPHERAL NODE ADDRESSIN IN NAIVE LYMPHOCYTE ADHESION TO HIGH ENDOTHELIAL VENULES IN A MUCOSAL SITE

Introduction

NALT represents the oropharyngeal lymphoid tissues of the upper respiratory airways (68, 69). This structure is believed to be analogous to human Waldeyer's ring (tonsils and adenoids) (72), and consists of bilateral lymphoid structures dorsal to the cartilaginous soft palate. It is thought, much like the PP, to behave as a mucosal inductive site. This resemblance is evident in both the organization and structure of NALT as well as its cellular composition. First, there is an epithelial layer overlaying the NALT which contains specialized "M" cells (68, 69) thought to mediate Ag entry much like that observed in the PP. There is a unique organization of both B cell zones and T cell areas much like that expected for the PP. In fact, the relative percentages of B and T cells in the NALT approximate those observed for the PP (75, 76, 83). While the NALT may not be the only site that contributes significantly to the stimulation of mucosal effector precursors for the upper airways, its importance may be due to its proximity to the nasal LP. Collectively, this evidence suggests that this unique structure is an important tissue for studying immunity to nasally-introduced antigens.

I.n. immunization is an effective route for stimulating mucosal immunity to a variety of pathogens (20, 21, 27, 28, 35), soluble proteins including CT (29, 30), and

microparticle-delivered Ags (83). This route of immunization induces strong antigen-specific mucosal and systemic IgA and IgG antibody responses (20, 27-30, 35, 83) and stimulates elevated CTL responses to viral and ovalbumin peptides (31, 33, 35). Thus, the elevations in humoral and cell-mediated immunity coupled with the ease of administering Ags make this a favorable route of immunization for local respiratory immunity, and immunity at distal mucosal sites (29, 30, 176, 177). In particular, i.n. immunization provides immunity in the genitourinary tract (27, 30, 32, 34, 65) where direct immunization is often hampered by epithelial cell turnover and hormonal influences. For instance, mice i.n.-immunized with the HIV gp160 protein produced HIV-1 neutralizing IgA and IgG antibodies in serum, lung, and vagina (27). Elevations in antigen-specific IgG and IgA were reported in vaginal secretions of mice following i.n. immunization with plasmid DNA as well as viral and bacterial vectors (21, 46, 65). While i.n. immunization may prove to be a highly effective method of inducing immunity in the genitourinary tract, it is unknown how immunization of the NALT leads to immunity at this distal mucosal site.

The ability of NALT to induce an immune response at a distal mucosal site may lie in part within the specialized ligands expressed by its HEV. These ligands, or "addressins", interact with specific homing receptors expressed by B and T lymphocytes and allow trafficking of the lymphocytes from blood into lymph tissue. However, the addressin profiles displayed by these HEV have yet to be identified, although some functional attributes of preferential homing by NALT lymphocytes have been observed. Lymphocytes isolated from rat NALT preferentially homed back to NALT, to CLN, and

to MLN rather than to the PP (125). This evidence suggests that the NALT addressin profile may differ from the PP.

Naive lymphocyte homing to the PP has been well characterized. It has been shown that MAdCAM-1 plays an important role in trafficking of naive B and T cells into PP (101, 178, 179). MAdCAM-1 is expressed in the PP, MLN, and in the gut LP (106, 112). Both B and T cells interact with MAdCAM-1 through the cellular ligand, $\alpha_4\beta_7$ (180). In some tissues, MAdCAM-1 also binds cells expressing L-selectin through the expression of the PNAd carbohydrate on the MAdCAM-1 glycoprotein backbone (101, 119). In contrast, naive lymphocyte trafficking into PLN is mediated by L-selectin binding to PNAd expressed on glycoproteins other than MAdCAM-1 (116, 122). Thus, there appears to be a definite separation between "mucosal" and "peripheral" type lymphocyte recirculation pathways, and it has yet to be determined whether NALT HEV express an exclusive mucosal or peripheral phenotype, or a combination of both.

In this study, we show that the NALT HEV express a unique addressin profile that resembles neither a strictly mucosal nor a peripheral phenotype. All NALT HEV express PNAd, either alone or in conjunction with MAdCAM-1. This unique profile differs greatly from the PP, the inductive site for the GALT. The functionality of this PNAd expression was explored through an *ex-vivo* binding assay, where lymphocytes bound to NALT HEV primarily through PNAd - L-selectin interactions. NALT lymphocytes also displayed unique expression of L-selectin profiles. In addition, NALT displayed both MAdCAM-1 and VCAM-1 on the follicular dendritic cells within its B cell areas. Finally, the relative location of HEV within the NALT differed greatly from

the PP. This study suggests that NALT is a unique mucosal tissue, where lymphocyte binding is primarily mediated by PNAd, and where the location of MAdCAM-1 and VCAM-1 expressed by FDC may play an important role in lymphocyte recruitment and retention.

Results and Discussion

Murine NALT HEV express a unique addressin profile

Lymphocyte trafficking into the PP requires MAdCAM-1 expression by its HEV (101, 179). If the NALT is indeed analogous to PP and behaves as a mucosal inductive site, it would be expected that its HEV would also mediate lymphocyte binding primarily through MAdCAM-1. To assess the NALT addressin phenotype, its HEV were examined for expression of both mucosal and peripheral addressins. NALT HEV were stained simultaneously with mAb for MAdCAM-1 (MECA 367 + TRITC labeled secondary) and PNAd (FITC conjugated MECA 79). The number of HEV expressing MAdCAM-1, PNAd, or both addressins in each NALT, PP, or MLN section was determined. As expected in a mucosal tissue, the NALT HEV expressed MAdCAM-1; however, the total percentage of HEV expressing mucosal addressin was significantly less than that observed in the PP (Figure 1: A-F, Table 2). In fact, all of the MAdCAM-1 positive HEV in the NALT also co-expressed PNAd. This co-expression was observed in 64.2% of the NALT HEV. No NALT HEV expressed MAdCAM-1 only. In contrast, 52.4% of PP HEV expressed MAdCAM-1 only, while the remaining 47.6% of PP HEV expressed MAdCAM-1 and PNAd ($p < .0001$). In addition, there was a significant difference in the number of HEV expressing PNAd alone in the NALT (37.2%) when

compared to MLN (2.5%) ($p < .01$). NALT also differs from the PLN, where nearly 100% of HEV express PNAd alone. Thus, NALT HEV express a unique addressin profile, one that differs from the strictly peripheral phenotype of the PLN, as well as from the intestinal PP and MLN HEV addressin profiles.

Table 2. Percentages of MAdCAM-1, PNAd, and double positive HEV^a in NALT, PP, MLN and PLN

Tissue	<i>n</i>	MAdCAM-1 only positive	PNAd only positive	Double positive
PP	147	52.4 ± 6.4	0	47.6 ± 6.4
MLN	343	40.9 ± 4.8	2.5 ± 0.9	56.8 ± 4.6
NALT	921	0	37.2 ± 5.0	62.8 ± 5.0
PLN	209	0	95.5 ± 2.0	4.5 ± 2.0

^aValues are expressed as the percentage of HEV expressing MAdCAM-1 alone, PNAd alone, or double positive/total number of HEV per node. SEM reported.

Staining of NALT sections with MECA 367 revealed diffuse MAdCAM-1 located within the B cell area of the NALT as well as on HEV (Figure 2: I, M.). Staining for VCAM-1 showed localization within the B cell areas, but not on HEV within the NALT (Figure 2 Q). However, staining for MAdCAM-1 in the NALT consistently appeared very diffuse, while staining for VCAM-1 appeared very intense. This staining profile differed greatly from the PP, which showed dark staining with the anti-MAdCAM-1 antibody (Figure 2: G, K). In addition, NALT FDC displayed different addressin

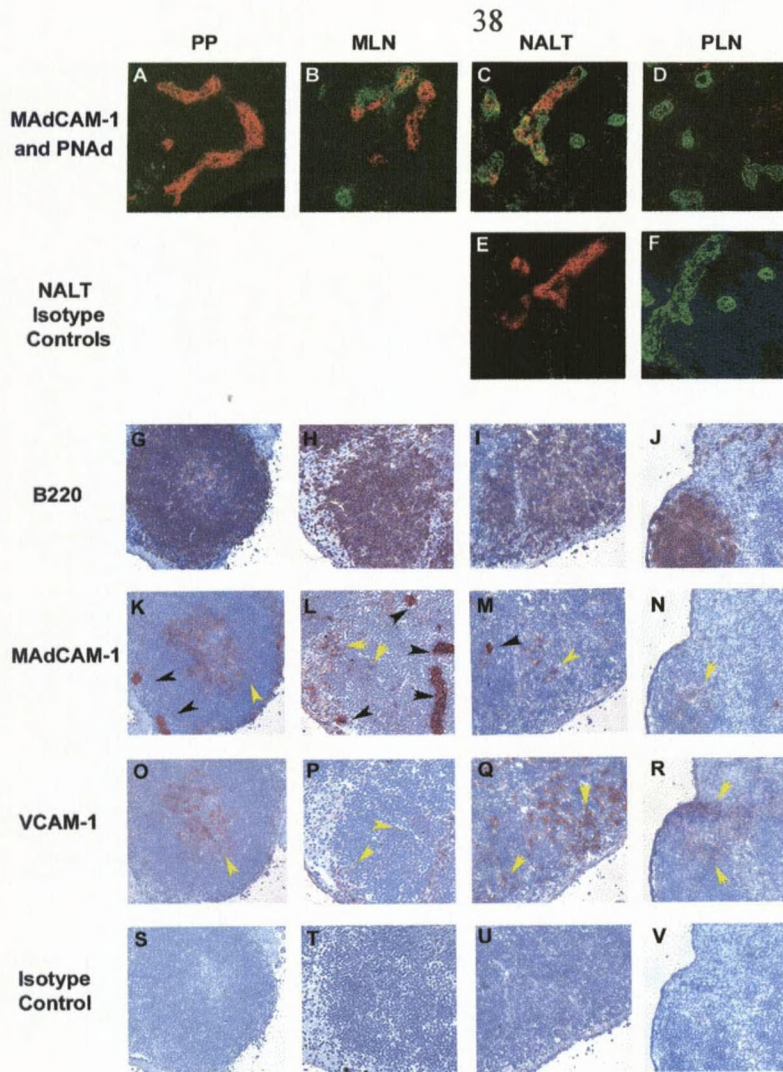


Figure 2. (A-F) Murine NALT HEV display an addressin phenotype different from PP. Fixed tissue sections were treated with MECA 367 + TRITC conjugated goat anti-rat IgG (red color) and FITC conjugated MECA 79 (green color). Results are visualized at 180X magnification, and images were captured using a Spot digital imaging system (Diagnostic Instruments, Inc. Sterling Heights, MI). Red and green images were overlaid to produce the double positive images shown in A-D. Negative isotype-matched controls are shown for the NALT tissue, where the MECA 367 + anti-rat TRITC was followed by treatment with a FITC labeled irrelevant IgM isotype control (E), or an IgG2a isotype control + anti-rat TRITC was followed by treatment with MECA 79 FITC (F). (G-V) NALT FDC display both MAdCAM-1 and VCAM-1. NALT, PP, and PLN serially cut frozen sections were treated with anti-B220 in order to visualize the B cell areas (G-J) with an AEC substrate (red color). Results are visualized at 200X magnification. The same areas were then observed for diffuse staining with MECA 367 (K-N) or anti-VCAM-1 (O-R) antibodies. Black arrows denote HEV staining, while yellow arrows indicate diffuse addressin staining. Specificity of staining is shown by treatment of the tissues with an irrelevant IgG2a isotype control (S-V).

profiles from MLN, which showed very little VCAM-1 staining and a higher incidence of MAdCAM-1. In contrast, although PLN displays VCAM-1 on its FDC, very little MAdCAM-1 staining is observed in the follicles (Figure 2: J, N, R). Taken together, these Ab stains provide further evidence for the expression of a unique addressin profile in the NALT.

Initial naive lymphocyte binding to NALT HEV is mediated primarily by PNA_d-L-selectin interactions

In order to determine if the PNA_d expressed by NALT HEV is functional, we utilized a Stamper-Woodruff *ex vivo* binding assay. Frozen tissue sections were treated with mAbs specific for MAdCAM-1, PNA_d, or with irrelevant isotype matched antibodies. For blocking of cellular homing receptors, naive MLN lymphocytes were pretreated with mAbs specific for the $\alpha_4\beta_7$ or L-selectin, or with a rat IgG2a isotype control antibody. The number of cells bound/HEV/node in the presence of addressin-specific antibody was compared to control binding, defined as lymphocytes bound to HEV in the presence of isotype-matched control antibody. Blocking of the PNA_d expressed on the HEV of NALT with the MECA 79 antibody resulted in a 60% reduction of binding when compared with control (Figure 3). This reduction of lymphocyte binding was similar to that observed in peripheral lymph node sections treated with MECA 79. In contrast, treatment of PP with MECA 79 resulted in no significant reduction in naive lymphocyte binding ($p < 0.01$). Treatment of NALT HEV with MECA 367 antibody had little effect ($< 20\%$) upon the number of lymphocytes bound/HEV, indicating that the expressed MAdCAM-1 has no apparent role in naive

lymphocyte binding. These results were in direct contrast with PP, where treatment of sections with MECA 367 resulted in greater than 90% reduction in binding. In addition, NALT HEV displayed no similarities in binding to MLN HEV as 50% of naive lymphocyte binding to MLN was blocked by MECA 367. Thus, initial naive lymphocyte binding to NALT HEV was most similar to naive lymphocyte binding to peripheral lymph node HEV, and was dissimilar to the binding observed in the PP, again providing evidence that NALT acts in a manner unique from other characterized mucosal tissues.

Blocking of naive lymphocyte homing receptors provided further evidence that the NALT HEV displayed a more peripheral addressin phenotype (Figure 4). Blocking of L-selectin using MEL-14 resulted in a > 90% reduction in binding of naive lymphocytes to NALT HEV. Binding of lymphocytes to NALT HEV was reduced to a lesser extent by blocking of $\alpha_4\beta_7$ with FIB 30, which reduced binding by about 60% when compared with controls. MEL-14 blocking of naive lymphocyte binding to NALT was similar to that observed in the PLN, where this antibody blocked nearly all naive lymphocyte binding. However, as expected, treatment with FIB 30 antibody had no effect on binding in the PLN. In the PP, MEL-14 reduced binding of naive lymphocytes to HEV by approximately 30% when compared with controls ($p < 0.01$), while the FIB 30 antibody showed a > 90% reduction in naive lymphocyte binding ($p < 0.0001$). In the MLN, naive lymphocytes exhibit characteristics of binding to both mucosal and peripheral addressin, evidenced by an approximately 80% reduction in binding by both FIB 30 and MEL-14 ($p < 0.01$). These results suggest that the NALT HEV express a unique addressin phenotype, and that naive lymphocyte binding to NALT HEV is

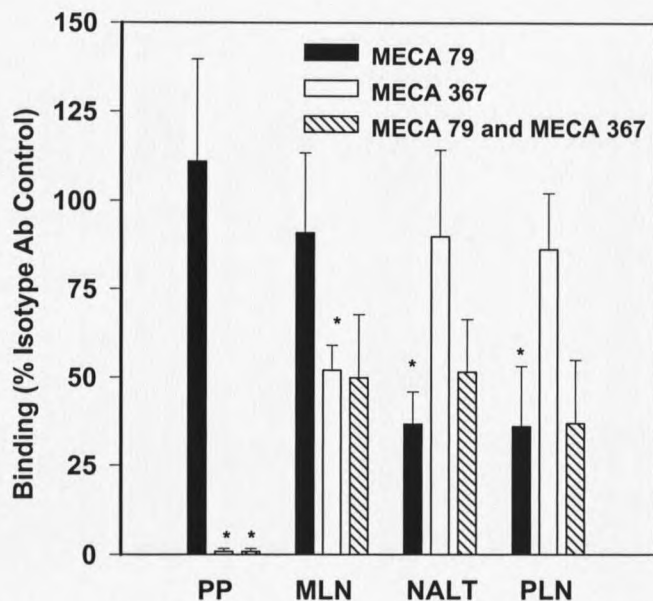


Figure 3. An anti-PNAd Ab blocks initial naive lymphocyte binding to NALT HEV. Fresh tissue sections were treated with 50 μ g/ml of MECA 79 (anti-PNAd), MECA 367 (anti-MAdCAM-1) mAbs or purified rat IgG2a, or IgM isotype matched Ab control for one hour before the addition of MLN lymphocytes. The average number of lymphocytes binding/HEV in each node was determined. Lymphocyte binding is expressed as the percentage of the numbers of cells bound/HEV in the presence of a non-specific isotype matched control Ab. 10-20 HEV/node were counted in each tissue type, and an average of 7.5 lymphocytes were bound/HEV on isotype control treated sections. MECA 79 mAb blocked > 60% of naive lymphocyte binding to both NALT and PLN HEV, but not to PP HEV. The indicated values are the mean of three experiments \pm SEM. * $p < 0.01$

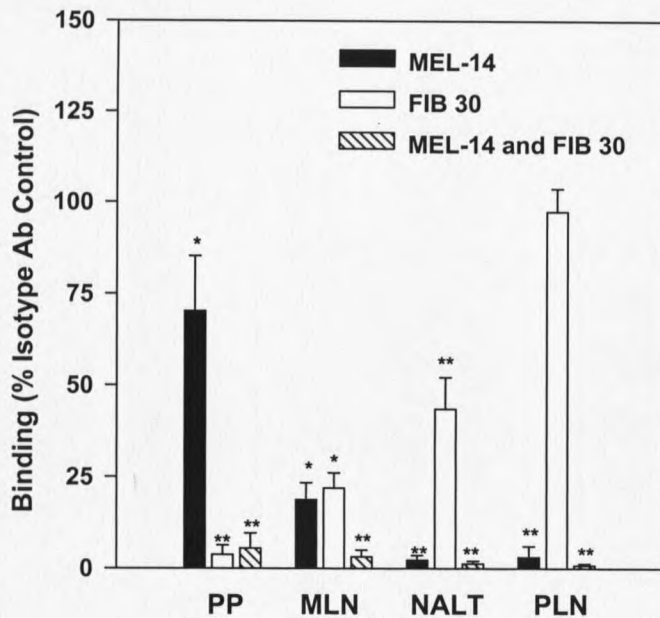


Figure 4. An anti-L-selectin Ab blocks initial naive lymphocyte binding to NALT HEV. MLN lymphocytes ($10^7/\text{ml}$) were treated with $50 \mu\text{g}/\text{ml}$ of purified MEL 14 (anti-L-selectin) mAb, FIB 30 (anti- β_7) mAb, or purified rat IgG2a, isotype matched Ab control for 30 minutes before their addition to tissue sections. The average number of lymphocytes binding/HEV in each node was determined. Lymphocyte binding is expressed as the percentage of the numbers of cells bound/HEV in the presence of a non-specific isotype matched control Ab. 10-20 HEV/node were counted in each tissue type, and an average of 6.5 lymphocytes were bound/HEV on isotype control treated sections. MEL 14 mAb blocked > 90% of naive lymphocyte binding to both NALT HEV, but had a negligible effect on naive lymphocyte binding to PP HEV. The indicated values are the mean of three experiments \pm SEM. * $p < 0.01$ ** $p < 0.0001$

primarily mediated by L-selectin - PNAd interactions. However, $\alpha_4\beta_7$ - MAdCAM-1 interactions may also play a role, as evidenced by the reduction in binding observed upon treatment of naive lymphocytes with FIB 30 antibody. These data are in contrast to the pattern observed in PLN HEV, where initial binding is blocked almost completely by MEL-14, but not by FIB 30. These results were consistent with the NALT phenotype, in which all HEV are decorated with PNAd, unlike PP HEV. NALT HEV mediated initial naive lymphocyte binding through different addressin-receptor pairs than did PP HEV. Thus, NALT HEV expressed a more "peripheral" phenotype, both in form and in function. Lymphocyte binding to the NALT primarily through PNAd rather than MAdCAM-1 suggested that the profiles of $\alpha_4\beta_7$ and L-selectin expression on the B and T cells of the NALT might be different from those observed in the PP as well.

NALT lymphocytes express a unique L-selectin profile

Based upon the observation that naive lymphocyte binding to NALT HEV was primarily mediated by L-selectin - PNAd interactions, it would be expected that NALT lymphocytes express profiles of L-selectin expression more similar to PLN than to PP lymphocytes. Two color flow cytometry analyses of lymphocytes isolated from NALT, PP, and PLN were performed to determine the expression of L-selectin on B cells, CD4⁺ T cells, and CD8⁺ T cells (Figure 5). As expected for naive lymphocytes, nearly all of the NALT B and T cells expressed L-selectin, similar to the L-selectin⁺ populations observed in the PLN. This result differed from the PP where a significant portion of the B220⁺ and CD4⁺ lymphocytes were L-selectin⁻ (Figure 5, Table 3).

observed in the PLN. This result differed from the PP where a significant portion of the B220⁺ and CD4⁺ lymphocytes were L-selectin⁻ (Figure 5, Table 3).

The NALT L-selectin⁺ lymphocyte homing receptor profile appeared to more closely resemble that of a PLN rather than a PP, and these data substantiated the results of the *ex vivo* binding assays, where initial binding was mediated primarily through L-selectin interactions with PNAd.

Table 3. Comparison of the percentages^a of NALT, PP, PLN^b, and MLN^c B and T lymphocytes that express L-selectin.

	<i>PP</i>	<i>MLN</i>	<i>NALT</i>	<i>PLN</i>
B220 ⁺	71.2 ± 3.7	87.0 ± 2.3	86.7 ± 2.6	96.9 ± 0.4
CD4 ⁺	60.2 ± 2.9	88.7 ± 0.6	89.3 ± 1.5	94.8 ± 0.8
CD8 ⁺	62.7 ± 8.5	92.9 ± 0.2	87.2 ± 4.5	94.3 ± 1.6

^aPercentage of NALT, Peyer's patch (PP), peripheral lymph node (PLN), and mesenteric lymph node (MLN) B220⁺, CD4⁺ and CD8⁺ lymphocytes expressing L-selectin.

^b average values for NALT, PP, and PLN from 9 experiments.

^c average values for MLN from 3 experiments ± SEM reported.

Segregation of double positive and PNAd positive NALT HEV in B and T cell areas

Although van der Ven and Sminia had observed HEV within the T cell areas of murine NALT (69), the expressed mucosal and peripheral addressins had not yet been fully characterized. It was therefore unknown if the various HEV phenotypes unique to the NALT segregated to specific B cell zones or T cell areas within the tissue.

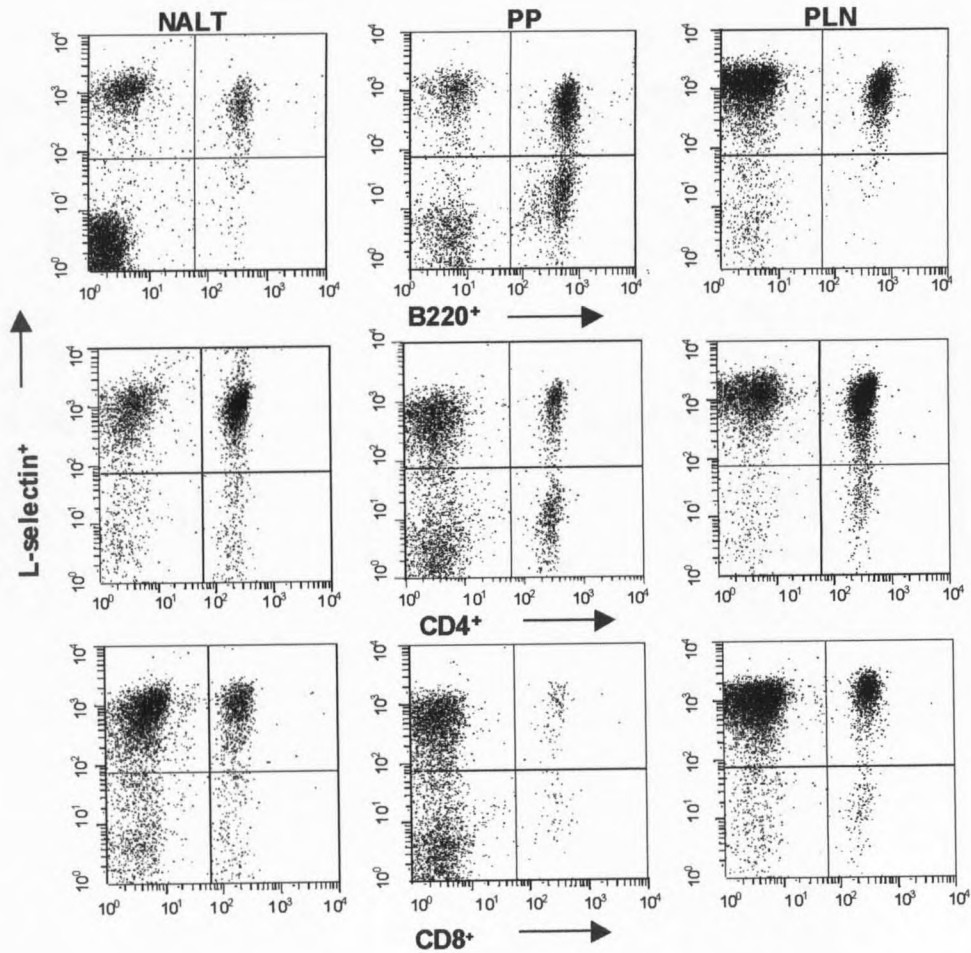


Figure 5. Expression profiles of L-selectin on NALT resemble PLN. NALT, PP, MLN, or PLN lymphocytes were treated simultaneously with FITC conjugated anti-B220, anti-CD4, or anti-CD8 mAbs and PE-conjugated anti-L-selectin (MEL-14) mAb. Representative plots are shown for each tissue. As depicted, the majority of NALT and PLN lymphocytes are L-selectin⁺, in contrast to the PP, which contained both L-selectin⁺ and L-selectin⁻ lymphocyte populations.

In order to determine if the location of HEV within the NALT affected the type of addressin expressed a sequential double immunoperoxidase staining was performed. Staining of murine NALT with anti-B220 and anti-CD3 monoclonal antibodies showed clearly defined B and T cell regions. HEV were localized to both the T and B cell regions (Table 4): 39.7% of HEV that expressed PNAd were located in the B cell areas, while the remaining PNAd⁺ HEV (58.6%) were located within the T cell areas. No significant difference was observed for the distribution of NALT HEV co-expressing PNAd and MAdCAM-1 in the B and T cell areas. In addition, our evidence also suggests that these double positive HEV were more likely to be located within the B cell areas of the NALT, than were the HEV expressing PNAd alone ($p = 0.05$). However, in comparison to the PP, in which only 16.2% of double positive HEV were located in the B cell areas, a significantly greater number of NALT double positive HEV were located within the B cell area ($p < .001$) (Table 4).

Murine NALT is a unique mucosal inductive site

We have shown that murine NALT HEV express a unique addressin phenotype. All NALT HEV expressed either PNAd alone, or co-expressed PNAd with MAdCAM-1. The addressin profile expressed by NALT HEV is considerably different from that expressed by the HEV of the gut mucosal inductive tissue, the PP. In addition, strong staining with a monoclonal antibody against VCAM-1 was observed in the FDC of NALT. Together, these results suggest that although NALT behaves as a mucosal inductive site like the PP, it displays a unique addressin profile, much different from the

Table 4. Locations^a of Double and Single Positive HEV within NALT and PP^b

	B cell area	T cell area
NALT HEV		
Double positive	57.4 ± 8.3	40.9 ± 7.9
PNAd positive	39.7 ± 3.8	58.6 ± 3.7
PP HEV		
Double positive	16.2 ± 4.4	74.5 ± 8.0
MAdCAM-1 positive	19.1 ± 4.5	81.0 ± 4.5

^a The number of HEV expressing either PNAd or MAdCAM₇-1 (indicated with DAB substrate) and their relative locations in the B cell zones or T cell area (indicated with VIP substrate) in the NALT were determined. The number of HEV/phenotype/area was divided by the total number of HEV/phenotype.

^bSEM reported for the average of the results from 12 sections.

PP expression of MAdCAM-1

Our results show that naive lymphocytes from nonimmunized mice bind to the NALT HEV using a peripheral addressin - homing receptor pair. The mucosal ligand - addressin $\alpha_4\beta_7$ - MAdCAM-1 interactions mediate both naive and memory lymphocyte homing to the PP and extralymphoid mucosal sites such as the gut lamina propria (178, 181). L-selectin also plays a role in naive lymphocyte trafficking into the PP (101), and this can be observed in the results of the *ex vivo* binding assay, where treatment of lymphocytes with MEL-14 reduces binding to PP HEV (Figure 4). Almost all naive lymphocytes display L -selectin on their cell surface, and thus are able to traffic throughout many different lymphoid sites in the body through interactions with PNAd. NALT HEV may express PNAd in order to facilitate naive lymphocyte trafficking through the nasal passages. Thus, naive lymphocytes can readily circulate through the lymphoid tissue that first encounters nasally introduced Ag.

However, this model does not readily explain why all NALT HEV express PNAd. In this respect, NALT more resembles a PLN than a PP. Several experiments have shown that lymphocyte homing to the upper airways of humans and sheep does not appear to be mediated primarily by $\alpha_4\beta_7$ -MAdCAM-1 interaction (152-154). Also, MECA 79 blocks naive lymphocyte binding to HEV of human tonsils (124). Intranasal immunization induces B cells that have both L-selectin and $\alpha_4\beta_7$ on their cell surface, in contrast to oral immunization, which induces mainly $\alpha_4\beta_7$ expressing B cells (182). In addition, i.n. immunization has been shown to be far more effective than oral immunization at producing protective immune responses in the lower respiratory tract

(176, 177). This may reflect a specific homing pathway of effector cells induced in the NALT rather than the PP. It appears as though L-selectin - PNAd interactions may be most important for lymphocyte trafficking into the respiratory tract, and this conclusion is reflective of the addressin profile of the NALT HEV. Since the respiratory tract contains both mucosal (upper airways and bronchi) and systemic (alveolar spaces) compartments, the co-expression of a peripheral phenotype with the mucosal addressin may enable trafficking of lymphocytes that facilitate both systemic and mucosal immune responses.

The presence of MAdCAM-1, VCAM-1, and PNAd within the NALT presents interesting implications for the theory of the "common mucosal immune system." Recent studies have shown that $\alpha_4\beta_7$ - MAdCAM-1 interactions do not appear to play a major role in lymphocyte trafficking into the lung or pulmonary tissues (124, 153, 154, 182), but do provide a mechanism for protective immunity against gut pathogens (151). Therefore, it has been suggested that this addressin/homing receptor pair should be regarded as "intestinal" rather than "mucosal" (183). However, our studies in the mouse suggest $\alpha_4\beta_7$ - MAdCAM-1 interactions may play some role in the recruitment of lymphocytes to the nasal tissues, and may thus provide a method of dissemination of Ab producing cells to distal mucosal effector sites, including the intestinal and reproductive tracts.

$\alpha_4\beta_7$ - MAdCAM-1 interactions may also play a role in the initial binding of naive lymphocytes to NALT HEV. This is evidenced by a 60% reduction in binding in lymphocytes treated with the anti- β_7 antibody FIB 30 (Figure 4). These data suggest a mechanism for the entrance of intestinal lymphocytes, which have been shown to

preferentially express $\alpha_4\beta_7$ and enter lymphoid tissue primarily through MAdCAM-1 - $\alpha_4\beta_7$ interactions (106, 178). Alternatively, the $\alpha_4\beta_7$ - MAdCAM-1 interaction may play a significant role in tight adhesion of lymphocytes to NALT HEV. In the three step model of lymphocyte homing, the initial binding of lymphocytes to NALT HEV may be primarily mediated by L-selectin - PNAd interactions, while subsequent tight binding might be mediated primarily by MAdCAM-1 - $\alpha_4\beta_7$ interactions (101, 178).

The $\alpha_4\beta_7$ - MAdCAM-1 interaction also may play a significant role in the trafficking of memory lymphocytes to NALT. Memory lymphocytes preferentially express $\alpha_4\beta_7$ and home to MAdCAM-1 in the mucosal PP and LP (149, 150). In addition, MAdCAM-1 is upregulated in inflamed mucosal tissue (148, 178, 184). It has yet to be determined, however, if MAdCAM-1 is upregulated on the HEV of inflamed NALT, and if such an upregulation would result in a higher percentage of lymphocytes binding through $\alpha_4\beta_7$ interaction.

Another method for naive lymphocyte recruitment and/or retention in NALT is suggested by the expression of MAdCAM-1 and VCAM-1 by the FDC in the NALT. MAdCAM-1 expression on PP FDC has been recently characterized (145). MAdCAM-1 expression within the PP follicles could mediate binding by $\alpha_4\beta_7^+$ memory lymphocytes, while binding to the follicles of PLN appeared to be primarily mediated by VCAM-1 - $\alpha_4\beta_1$ interaction. It has also been shown (147) that VCAM-1 interactions with the α_4 subunit can mediate binding to the germinal centers of human tonsil. However, VCAM-1 also binds both $\alpha_4\beta_7$, as well as $\alpha_4\beta_1$ expressing lymphocytes (185), suggesting that the $\alpha_4\beta_7^+$ lymphocytes might bind in the germinal centers through this route as well. In

addition, adhesion to VCAM-1 may prevent apoptosis and allow for positive selection of B cells within the follicle (146). Although binding studies of lymphocytes to the NALT follicles have yet to be undertaken, the presence of relatively high levels of VCAM-1 within the NALT suggests that lymphocytes expressing both $\alpha_4\beta_7$ and $\alpha_4\beta_1$ integrins are able to traffic into these germinal centers where they then mature and differentiate.

Finally, our results indicated that in comparison to the PP, a greater percentage of the NALT HEV were located within the B cell areas. It appeared as though expression of MAdCAM-1 correlates with location of NALT HEV as well, as more double positive than single positive HEV were found within the B cell areas. The reason for this apparent localization of the HEV is unclear, but the localization of the HEV that can support binding of $\alpha_4\beta_7^+$ in the B cell area might provide a new mechanism for the localization of B cells to the B cell areas. Rather than entering the lymphoid tissue in the paracortex and migrating to the B cell areas in response to chemotactic factors, as has been recently reported (186), these lymphocytes might simply enter the B cell areas directly, where the MAdCAM-1 and VCAM-1 expression on dendritic cells might also enable B cell survival and differentiation. However, if T lymphocytes enter these B cell areas as well, some type of migration would still occur.

In summary, characterization of addressin expression revealed that NALT HEV were phenotypically and functionally distinct. This addressin profile was demonstrated to be important for initial naive lymphocyte binding mediated by PNAd expressed by NALT. Lymphocytes isolated from the NALT also displayed a homing receptor profile that more closely resembled lymphocytes derived from peripheral tissues. Finally, the

location of the HEV within the NALT differed dramatically from that observed in the PP. Collectively, these results suggest that NALT is a truly unique inductive mucosal tissue that cannot be equated with the intestinal PP. These data provide evidence for a unique lymphocyte homing pathway, where T and B cells activated in the NALT are able to preferentially circulate to alternate mucosal tissues.

CHAPTER 4

MAdCAM-1 EXPRESSION AND NAIVE LYMPHOCYTE BINDING
INTERACTIONS VARY AMONG THE CONALTIntroduction

Intranasal (i.n.) immunization offers a productive means for inducing mucosal immunity at local and distal mucosal tissues. Eliciting effective local immunity in the nasal cavity is possible because of the proximity of the draining LN where initial encounters between Ag and lymphocytes occur. These tissues support the induction of immunity in the oral cavity and associated salivary glands and are collectively referred to as the cranial, oral, and nasal-associated lymphoid tissues (CONALT). The CONALT encompasses the facial or parotid gland LN (PRLN) located posterior to the parotid gland, the submaxillary gland LN (SMLN), commonly referred to as the superficial cervical LN located anterior to the submaxillary gland (SMG), and the deep cervical LN (CLN) located dorsal to the brachial plexus deep within the musculature of the neck (60). The role of CONALT has been determined through i.n. immunization studies with soluble proteins, microparticles, and bacterial Ags. From these studies, it appears that the SMLN drain the nasal submucosa while the CLN drain the NALT (60, 86, 87), the SMLN, and the brain (88, 89). In contrast, the PRLN appear to be important for draining the skin of the head and neck as well as the conjunctiva (78, 85).

Salivary IgA responses can be stimulated via various modes of immunization (75, 187, 188). While oral immunization can induce specific salivary Abs, i.n. immunization

appears to be more efficient at stimulating sustained, elevated salivary immune responses (92). This effect is also evident in the CONALT where i.n. and, to a lesser extent, oral immunization with bacterial protein Ags coupled to CT-B produces strong IgA and IgG responses in the SMLN and CLN, resulting in immune S-IgA Abs in saliva (78). IgG responses in the PRLN are more effectively stimulated by s.c. rather than i.n. immunization. Furthermore, i.n. immunization with polymer microparticles induces IgG production in both the SMLN and the CLN (83), the latter having proven to be important in the triggering of allergic responses to particulate Ags (93) and to produce strong CTL responses after i.n. HIV peptide immunization (33). Though CONALT consists of lymph nodes from a similar area in the neck, immunization studies show that the responses of these LN can differ vastly depending on the route of immunization.

Varied immune responses in CONALT may be due to different addressin-homing receptor interactions in SMLN, PRLN, and CLN. Lymphocyte trafficking to intestinal sites is mediated by mucosal addressin cell MAdCAM-1 - $\alpha_4\beta_7$ interactions and PNAd-L-selectin interactions (101, 178, 179). The MAdCAM-1 glycoprotein is primarily expressed on HEV of the PP, the MLN, the intestinal LP, and in the minor vessels in the marginal sinus of the spleen (106, 112-114). MAdCAM-1 - $\alpha_4\beta_7$ interactions mediate both the initial tethering and tight binding interactions in the three-step model of lymphocyte homing (101). MAdCAM-1 also binds to L-selectin through expression of the PNAd carbohydrate on the MAdCAM-1 glycoprotein backbone (101, 119). In contrast, lymphocyte trafficking to the lungs appears to be rely on peripheral, rather than mucosal addressin - homing receptor interactions (122, 153). Initial naive lymphocyte

binding in the peripheral sites takes place through the interaction of PNAd with its cellular ligand, L-selectin (122, 123). PNAd, defined as several different carbohydrate epitopes recognized by the MECA 79 mAb, is predominantly expressed on glycoprotein backbones other than MAdCAM-1 on the HEV of peripheral LN (116). Interestingly, HEV in the mucosal inductive site for the upper airways, NALT, also primarily expresses PNAd (189). It is unknown what addressin-homing receptor interactions mediate naive lymphocyte trafficking to the salivary gland and associated LN; however, studies of lymphocyte homing receptors in the rat SMG revealed that $\alpha_4\beta_7$ and as a high percentage of L-selectin was expressed on SMG lymphocytes (190). To date, the addressin-homing receptor interactions in the CONALT have not been defined in detail.

In this study, we show that the addressin profiles expressed on the HEV of the SMLN, CLN, and PRLN more closely resemble those of peripheral LN rather than intestinal tissues. Significantly, the majority of lymphocyte binding to these tissues is mediated primarily by PNAd-L-selectin interactions. However, important differences in addressin expression and lymphocyte binding exist among the CONALT, as the PRLN appear more peripheral due to lymphocyte binding mediated by PNAd-L-selectin interactions. In contrast, the CLN appear to be relatively more mucosal with some lymphocyte binding mediated by MAdCAM-1- $\alpha_4\beta_7$ interactions. These experiments suggest the importance of peripheral addressin-homing receptor interactions in the CONALT, while indicating the role that varied expression of addressins plays in the functions of LN.

Results and Discussion

The CONALT display different addressin phenotypes

It has been postulated that Ag-specific lymphocytes disseminate from the NALT to the CONALT, which eventually provides effector IgA B cell immunity in the salivary glands and NP (60, 81, 83, 78, 91). If this is the case, it would be expected that the CONALT might express the same addressin phenotype as the NALT. To assess the addressins expressed on the HEV of the SMLN, PRLN, and CLN, double immunofluorescent staining with anti-MAdCAM-1 (MECA 367) and anti-PNAd (MECA 79) mAbs was performed (Fig. 6). Results from the immunostaining revealed that the CONALT expressed a variety of mucosal and peripheral addressin phenotypes. Most importantly, the CLN expressed a more mucosal phenotype than did the SMLN or PRLN. The majority (63%) of HEV in the CLN expressed PNAd, and 24% also co-expressed MAdCAM-1 (Figure 6 C, Table 5). HEV in the CLN expressing MAdCAM-1 alone were limited to only 8%. These results contrasted with the addressin phenotypes observed on the HEV of the SMLN and PRLN, which appeared more peripheral-like. In the SMLN, 86% of HEV expressed PNAd alone; 10% expressed both MAdCAM-1 and PNAd, and less than 1% of HEV expressed MAdCAM-1 alone (Fig. 6 B, Table 5). Of the three LN, the PRLN appeared to be the most peripheral, since 93% of its HEV expressed PNAd alone, 6% co-expressed MAdCAM-1, and approximately 1% of the HEV expressed MAdCAM-1 alone (Fig. 6 A, Table 5). Although these LN may drain related tissues, their varying addressin profiles might indicate selective trafficking of naive lymphocyte subsets.

Table 5. Percentages of MAdCAM-1, PNAd, and double positive HEV in PRLN, SMLN, and CLN^a.

Tissue	<i>n</i>	MAdCAM-1 positive	PNAd positive	Double Positive
PRLN	25	1.3 ± 1.3	92.9 ± 2.8	5.7 ± 2.6
SMLN	34	0.9 ± 0.5	85.8 ± 4.0	10.4 ± 3.1
CLN	18	7.6 ± 5.6	62.7 ± 10.0	24.2 ± 8.6

^a Mean values ± SEM are expressed as the percentage of HEV expressing MAdCAM-1, PNAd, or double positive/total number of HEV per node. PRLN from 13 mice, SMLN from 17 mice, and CLN from 9 mice were analyzed. *n* values represent the number of nodes analyzed.

Extravascular MAdCAM-1 and VCAM-1 are expressed within CONALT

Studies have shown that addressin expression by interfollicular dendritic cells and macrophages is important in lymphocyte recruitment and retention in LN (145, 147, 191). In order to determine additional addressins that might mediate lymphocyte binding in the CONALT, immunoperoxidase staining for non-vascular MAdCAM-1 and VCAM-1 was performed. Staining of CONALT tissue sections with MECA 367 mAb revealed intense staining for MAdCAM-1 in the follicular stromal elements in the CLN and SMLN (Fig. 6, G and H). In the CLN, this intense staining for diffuse MAdCAM-1 correlated with the expression of MAdCAM-1 on the HEV. In contrast, staining for diffuse MAdCAM-1 in PRLN, where less than 10% of HEV expressed MAdCAM-1, appeared considerably less intense (Fig 6 F). However, staining with the anti-VCAM-1 mAb in the PRLN revealed intense diffuse staining for VCAM-1 in the follicular and parafollicular regions

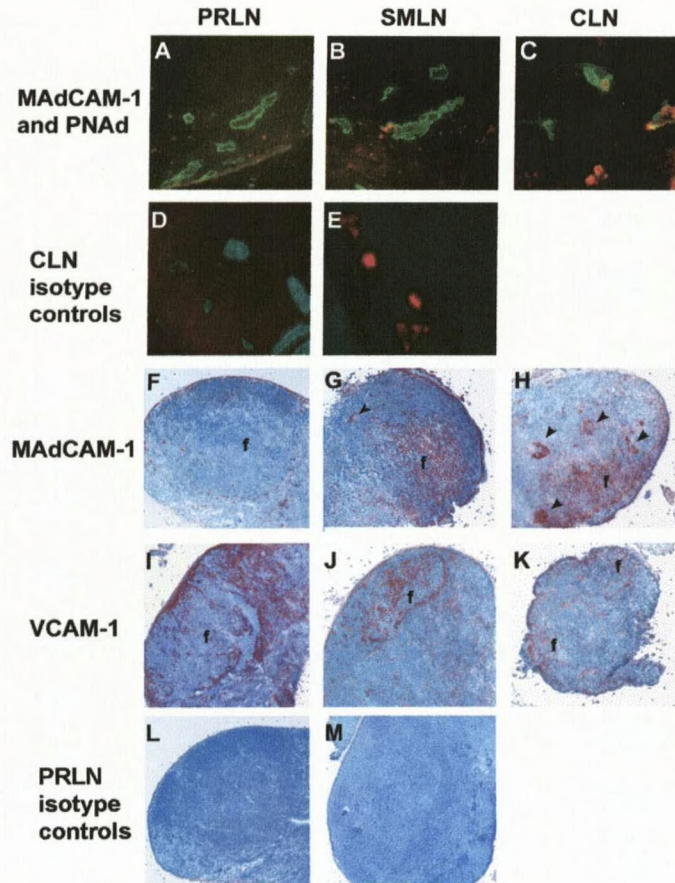


Figure 6. A-E, The CLN have a more mucosal phenotype than the SMLN or PRLN. Fixed tissue sections were treated with MECA 367 mAb TRITC conjugated goat anti-rat IgG (red color), and FITC conjugated MECA 79 mAb (green color). Results are visualized at 180X magnification, and images were captured using a Spot digital imaging system (Diagnostic Instruments, Inc). Red and green images were overlaid to produce the double positive images shown in A-C. Isotype matched negative controls are shown for the CLN, where a rat IgG2a isotype control and TRITC anti-rat IgG were followed by treatment with FITC MECA 79 mAb (D) or MECA 367 mAb, and TRITC-anti-rat IgG was followed by treatment with FITC-labeled irrelevant rat IgM isotype control (E). F-M, Extravascular MAdCAM-1 and VCAM-1 are expressed in CONALT. Immunohistochemical staining with MECA 367 mAb revealed MAdCAM-1 expression in the parafollicular region of PRLN (F) and in the follicles (denoted by "f") and on HEV (arrows) of the SMLN and the CLN (G-H). Intense VCAM-1 staining was observed in both follicular and medullary regions of PRLN (I), while lighter staining was observed in the same regions of the SMLN and CLN (J-K). Isotype matched negative control staining is shown for the PRLN, where nonspecific unlabeled (L) and biotinylated rat IgG2a (M) was added to sections, followed by secondary Ab and AEC development. PRLN are visualized at 26X magnification, while SMLN and CLN are magnified 50X.

of this node (Fig 6 I). The SMLN also displayed diffuse staining of VCAM-1 in the follicle, while CLN showed less intense VCAM-1 staining in its follicles (Fig 6 J and K). The varying expression of diffuse MAdCAM-1 and VCAM-1 among the CONALT supports the notion that the PRLN is the most peripheral of these nodes, while the CLN might be considered more mucosal. These results suggest differing patterns of lymphocyte retention in the CONALT tissues.

Naive lymphocyte binding to the HEV of the CONALT is mediated primarily by PNAd-L-selectin interactions

Since the HEV of the CLN displayed a more mucosal phenotype, we hypothesized that naive lymphocyte binding to this LN might be mediated by both MAdCAM-1- $\alpha_4\beta_7$ and PNAd-L-selectin interactions, while binding to the SMLN and the PRLN would be mediated almost exclusively by PNAd-L-selectin interactions. To investigate these possibilities, a modification of the Stamper-Woodruff *ex vivo* binding assay (174, 189) was performed using a sample population of cells isolated from MLN, which contain both L-selectin- and $\alpha_4\beta_7$ -bearing lymphocytes. These cells were rotated above tissue sections of PRLN, SMLN, or CLN in the presence of mAbs against $\alpha_4\beta_7$, L-selectin, MAdCAM-1, or PNAd, or in the presence of unrelated isotype -matched controls. Blocking of non-stimulated lymphocyte binding to the HEV of the nodes was measured as a percentage of cells/bound/HEV in the presence of blocking Abs versus cells/bound/HEV with isotype matched negative controls.

These experiments revealed that nearly all initial naive lymphocyte binding in CONALT is mediated primarily by PNAd-L-selectin interactions, though some

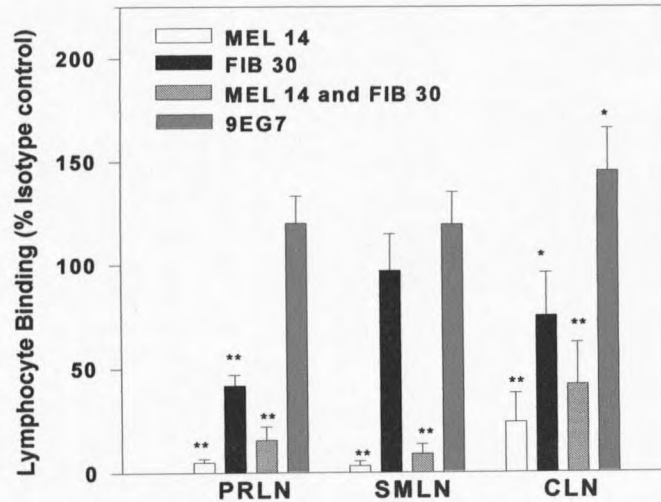


Figure 7. An anti-L-selectin mAb blocks initial naive lymphocyte binding to CONALT HEV. MLN lymphocytes ($10^7/\text{ml}$) were treated with $50 \mu\text{g}/\text{ml}$ of purified rat anti-mouse MEL-14 (anti-L-selectin) mAb, FIB 30 (anti- β_7) mAb, 9EG7 (anti- β_1) mAb, or purified rat IgG2a isotype control for 30 min prior to their addition over the tissue sections. The average number of lymphocytes bound/HEV in each node was determined. Lymphocyte binding is expressed as a percentage of the number of cells bound/HEV with treatment of a non-specific isotype-matched Ab. Two to twenty-two HEV were counted per node in each tissue type with an average of 10.2 cells bound/HEV in PRLN, 6.7 cells bound/HEV in SMLN, and 1.9 cells bound/HEV in CLN. MEL-14 blocked $> 95\%$ of naive lymphocyte binding to PRLN and SMLN HEV and approximately 90% of naive lymphocyte binding to CLN HEV. The 9EG7 mAb failed to block lymphocyte binding to any of the CONALT. The indicated values are the results of three experiments \pm SEM. * $p < 0.01$, ** $p < 0.0001$

interactions are mediated by MAdCAM-1- $\alpha_4\beta_7$. Treatment with the MEL 14 (anti-L-selectin) mAb blocked > 95% of lymphocyte binding to the PRLN and the SMLN ($p < 0.0001$) (Fig. 7) and approximately 75% of lymphocyte binding to the CLN ($p < 0.0001$). The FIB 30 (anti- β_7) mAb treatment of lymphocytes did not significantly reduce lymphocyte binding to SMLN, but it did reduce binding of lymphocytes to the HEV of the PRLN and the CLN by approximately 60% ($p < 0.0001$) and 40% ($p < 0.01$), respectively, indicating a possible role for MAdCAM-1- $\alpha_4\beta_7$ binding interactions in the HEV of these LN. In addition, since intense staining of VCAM-1 was noted in the PRLN and CLN, we performed blocking experiments with an anti- β_1 9EG7 mAb. However, no reduction in binding was observed, indicating that the $\alpha_4\beta_1$ integrin may have no role in initial naive lymphocyte binding to the CONALT. In fact, a significant increase in binding was observed in the CLN ($p < 0.01$). Identical results were observed with blocking with Ha2/5 anti- β_1 mAb (data not shown).

These results correlated with what was observed with the anti-addressin mAbs, MECA 367 (anti-MAdCAM-1), MECA 79 (anti-PNAd), and anti-VCAM-1 treatments of the CONALT (Fig. 8). In the CLN, MECA 79 and MECA 367 mAbs both blocked 40% of binding to HEV ($p \leq 0.02$). In the SMLN, MECA 79 mAb blocked 80% of binding to HEV ($p \leq 0.001$), while MECA 367 mAb had no effect on lymphocyte binding. Finally, in the PRLN, treatment with MECA 79 mAb reduced binding by nearly 40% ($p \leq 0.001$). While MECA 367 mAb had appeared to block some lymphocyte binding to this tissue, a paired Student's *t* test showed that this effect was not significant. However, treatment of PRLN with MVCAM.A mAb resulted in an approximately 45% reduction in lymphocyte

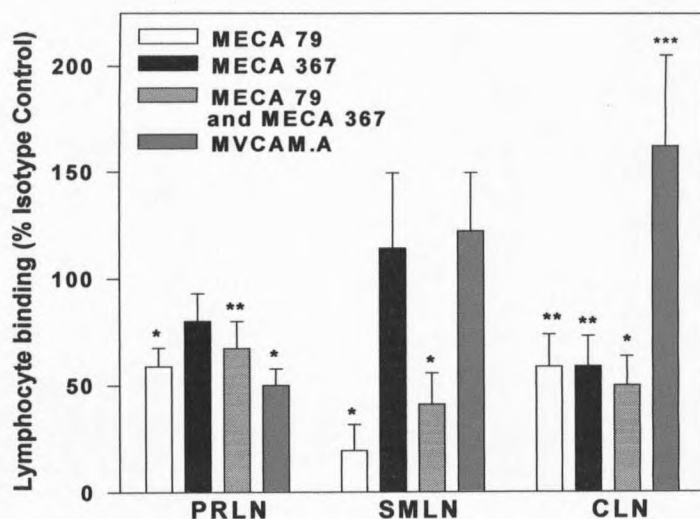


Figure 8. An anti-PNAd mAb blocks initial naive lymphocyte binding to the CONALT. Fresh tissue sections were treated with 50 $\mu\text{g/ml}$ MECA 79 (anti-PNAd), MECA 367 (anti-MAdCAM-1), or 50 $\mu\text{g/ml}$ purified MVCAM.A (anti-VCAM) mAb supernatant, or the same concentration of purified rat IgM or IgG2a isotype control for 1 hr prior to the addition of MLN lymphocytes. The average number of lymphocytes bound/HEV in each LN was determined. Lymphocyte binding is expressed as a percentage of the number of cells bound/HEV in the presence of a non-specific, isotype-matched control Ab. Two to twenty-two HEV were counted per node in each tissue type with an average of 11.7 cells bound/HEV in PRLN, 15.9 cells bound/HEV in SMLN, and 3.2 cells bound/HEV in CLN. MECA 79 (anti-PNAd) mAb blocked at least 40% of naive lymphocyte binding to the PRLN, SMLN, and the CLN, while MECA 367 (anti-MAdCAM-1) mAb blocked 40% of lymphocyte binding to the CLN only. Anti-VCAM-1 mAb blocked binding in PRLN only. The indicated values are the mean of three experiments \pm SEM. * $p \leq 0.001$, ** $p \leq 0.02$, *** $p = 0.03$.

binding ($p < 0.001$), correlating with the blocking observed with treatment of FIB 30 mAb. Although there appeared to be a significant amount of staining for VCAM-1 in the PRLN, an anti- β_1 mAb did not block binding. Since the ability of $\alpha_4\beta_7$ to bind VCAM-1 and MAdCAM-1 has been well documented (111, 185, 192), it is likely that $\alpha_4\beta_7$ binds to VCAM-1 in the PRLN as well as the small number of MAdCAM-1 positive HEV. This inhibition by the anti-VCAM-1 mAb was limited to the PRLN, since similar treatment did not significantly block binding in the SMLN or the CLN. Similar to the results observed with the anti- β_1 antibody, blocking of VCAM led to a significant increase in binding to CLN HEV ($p = 0.03$). Together, with evidence from the cell ligand blocking experiments, these results indicate that PNAd-L-selectin interactions mediate the majority of naive lymphocyte binding in the CONALT, with lesser roles for MAdCAM-1- $\alpha_4\beta_7$ and VCAM-1- $\alpha_4\beta_7$ interactions.

Lymphocytes of the CONALT primarily express L-selectin

Results from the Stamper-Woodruff assay suggested that since naive lymphocyte binding in the CONALT was primarily mediated by PNAd-L-selectin interactions, the percentages of L-selectin⁺ and $\alpha_4\beta_7$ ⁺ lymphocytes in the three LN might be similar as well. Three-color flow cytometry analyses of CONALT lymphocytes revealed that there was not a significant difference in the populations of L-selectin⁺ lymphocytes in these LN (Fig 9; Table 6). B220⁺ lymphocytes in the SMLN and CLN expressed slightly lower percentages of L-selectin (91%) than did the B220⁺ lymphocyte population in the PRLN (95%), but this difference was not statistically significant (Table 6). The CD4⁺

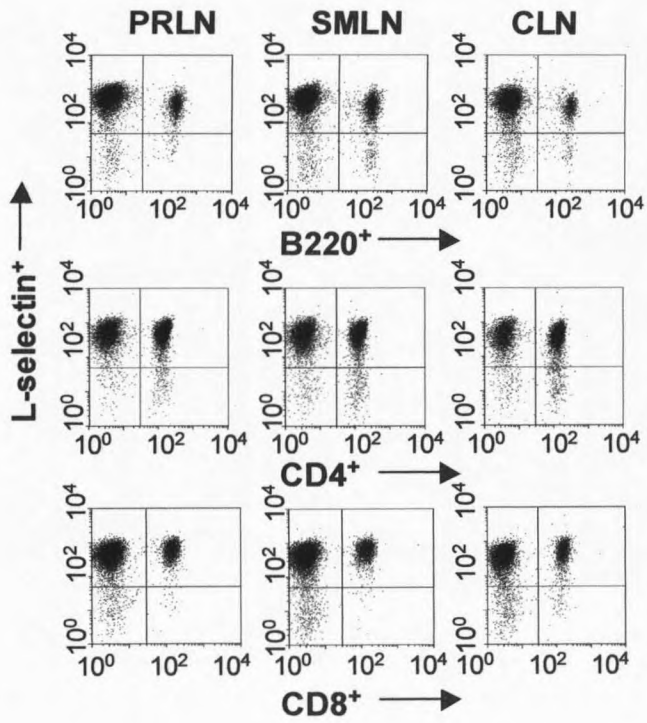


Figure 9. L-selectin is expressed on the majority of CONALT lymphocytes. Plots depict expression of L-selectin by B220⁺, CD4⁺, and CD8⁺ lymphocytes. Plots are representative of three experiments.

lymphocytes in the SMLN, PRLN, and CLN expressed slightly higher percentages of L-selectin (~ 95%) than did the B220⁺ lymphocytes. Finally, nearly all (97-98%) of the CD8⁺ lymphocytes in the CONALT expressed L-selectin. Here again, the percentage of L-selectin⁺, B220⁺, CD4⁺, and CD8⁺ lymphocytes did not vary significantly among the three LN.

Table 6. Comparison of percentage of B and T lymphocytes expressing L-selectin in the CONALT^a.

	PRLN	SMLN	CLN
B220 ⁺	95.2 ± 2.2	90.8 ± 1.6	90.6 ± 4.1
CD4 ⁺	95.9 ± 1.1	94.1 ± 1.6	95.0 ± 0.5
CD8 ⁺	97.1 ± 1.2	97.6 ± 0.8	97.2 ± 0.6

^aPercentage of PRLN, SMLN, and CLN B220⁺, CD4⁺, and CD8⁺ lymphocytes expressing L-selectin. Mean values ± SEM from three experiments, tissues were pooled from five mice in each experiment.

In contrast, lymphocytes in the CONALT expressed mostly low levels of $\alpha_4\beta_7$ (Table 7). B220⁺ lymphocytes expressed the highest percentage of $\alpha_4\beta_7$ in the CLN (86.6%), SMLN (81.8%), and PRLN (78%). The percentage of $\alpha_4\beta_7$ expression on CD4⁺ lymphocytes in the CONALT was much lower (46-50%), and 53-59% of CD8⁺ lymphocytes expressed $\alpha_4\beta_7$. However, $\alpha_4\beta_7^{\text{high}}$ lymphocytes were also found in CONALT (Fig. 10). Combined results from 5 experiments revealed that fifty percent of

$\alpha_4\beta_7^+$ B cells in the CLN were classified as high-expressing (Table 7), while only 33% and 37% of $\alpha_4\beta_7^+$ B cells in the SMLN and PRLN, respectively, were high-expressing. In addition, very few $\alpha_4\beta_7^{\text{high}}$ CD8⁺ cells (7-15%) were present in the CONALT. These results clearly show that the majority of lymphocytes that enter the CONALT are L-selectin⁺ and suggest that peripheral addressin-homing receptor interactions dominate in the CONALT, though some mucosal interactions may be important in CLN.

Table 7. Comparison of percentage of B and T lymphocytes expressing $\alpha_4\beta_7$ in the CONALT^a.

	PRLN	SMLN	CLN
B220 ⁺ total	78.0 ± 9.5	81.8 ± 4.3	86.6 ± 5.6
high	35.3 ± 11.0	32.7 ± 7.1	50.6 ± 5.8
CD4 ⁺ total	46.7 ± 11.8	46.6 ± 8.3	46.4 ± 9.1
high	7.3 ± 2.9	7.4 ± 3.7	8.4 ± 2.7
CD8 ⁺ total	53.8 ± 14.4	56.7 ± 6.8	59.2 ± 9.5
high	11.8 ± 5.1	10.0 ± 6.4	15.7 ± 3.3

^aPercentage of PRLN, SMLN, and CLN B220⁺, CD4⁺, and CD8⁺ lymphocytes expressing total $\alpha_4\beta_7$ and percentage of total $\alpha_4\beta_7^+$ lymphocytes that are $\alpha_4\beta_7^{\text{high}}$. Mean values ± SEM from three experiments, tissues were pooled from five mice in each experiment.

L-selectin primarily mediates in vivo homing of CONALT lymphocytes

Though the results of the Stamper-Woodruff assays indicated that the majority of lymphocyte binding to HEV of CONALT was mediated by L-selectin-PNAd interactions, it was possible that $\alpha_4\beta_7$ -MAdCAM-1 interactions might be important in the tight binding second step of the rolling process as well as in retention of lymphocytes.

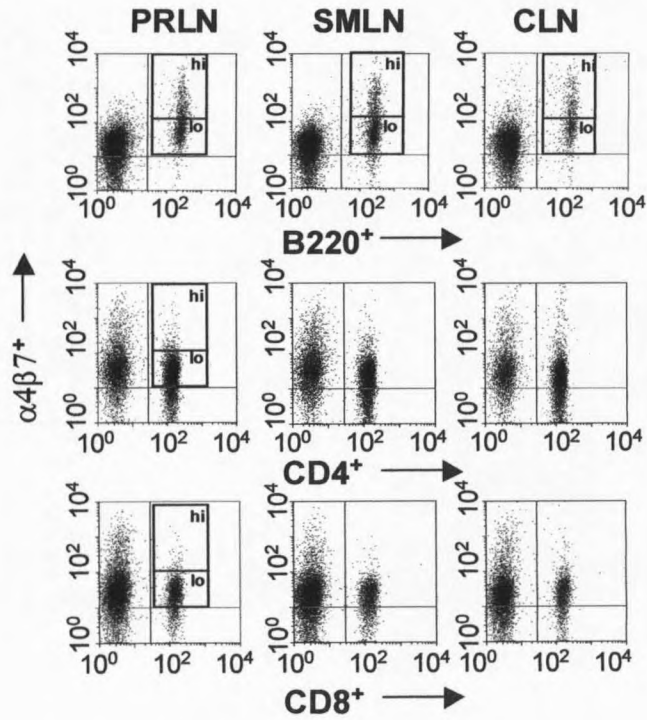


Figure 10. CONALT lymphocytes express primarily $\alpha_4\beta_7^{\text{low}}$. Plots depict expression of $\alpha_4\beta_7$ by B220⁺, CD4⁺, and CD8⁺ lymphocytes, and $\alpha_4\beta_7^{\text{low}}$ and $\alpha_4\beta_7^{\text{high}}$ populations are indicated for CONALT B lymphocytes and PRLN T lymphocytes. Plots are representative of three experiments.

Therefore, lymphocytes that bound to HEV via L-selectin-PNAd interactions might require $\alpha_4\beta_7$ to extravasate into the lymph node and/or remain there. In order to test this possibility we performed *in vivo* lymphocyte homing experiments using CONALT lymphocytes isolated from C57BL/6-GFP mice, which constitutively express enhanced GFP on all nucleated cell types (170). Use of these mice provided a ready source of GFP-expressing lymphocytes, thus reducing the number of donor mice required in these experiments, since cell mortality would not occur as a result of chemical labeling. Since the number of lymphocytes recovered from SMLN, PRLN, or CLN alone would be prohibitively small and require a vast number of donor mice, we combined lymphocytes from all CONALT for use in these experiments.

Studies of short term lymphocyte homing (4 hours post injection; Table 8) revealed that in the presence of nonspecific isotype control Ab, CONALT lymphocytes were collected in the spleen and a high percentage migrated to MLN, which expressed both PNAd and MAdCAM-1. The percentage of GFP⁺/total CONALT lymphocytes found in SMLN was significantly higher than the percentage of GFP⁺ CONALT lymphocytes found to have homed to the PP ($p = 0.02$), suggesting preferential trafficking to CONALT, rather than to the mucosal inductive sites. Fewer GFP⁺ lymphocytes trafficked to CLN, perhaps indicating selective trafficking of CLN B and T cells, which comprised a much lower percentage of the overall CONALT lymphocyte population, back to the CLN. Because of low cell yields from CLN, it was impractical to perform homing experiments with cells from this LN alone. Still, these results show a clear bias for CONALT lymphocytes to traffic selectively to the CONALT, rather than the other

mucosal inductive sites, NALT and PP.

Table 8. Percentages of control Ab treated, donor GFP⁺ lymphocytes^a found in mucosal and peripheral tissue 4 hours and 24 hours after injection.

Tissue	4 hours	24 hours
NALT	0.23 ± .07	0.37 ± .22
SMLN	0.52 ^b ± .17	0.77 ^c ± .13
PRLN	0.38 ± .24	0.73 ^c ± .15
CLN	0.30 ± .08	0.50 ± .35
PLN	0.50 ± .21	1.00 ± .30
SPL	1.22 ± .41	0.67 ± .15
MLN	0.46 ± .20	0.83 ± .20
PP	0.24 ± .05	0.30 ± .06

^aMean values of the percentages of GFP⁺ lymphocytes/total lymphocytes in tissues from five experiments.

^bPercentage of GFP⁺ lymphocytes is significantly higher than percentage of lymphocytes in PP. $p = 0.02$

^cPercentages of GFP⁺ lymphocytes are significantly higher than percentage of lymphocytes in NALT and PP. $p = 0.03$

In addition, these data reveal that the anti-L-selectin mAb MEL 14 significantly blocked nearly all lymphocyte homing to SMLN, PRLN, and CLN ($p < 0.001$; Fig 11 A), while the anti- β_7 mAb FIB 30 had no impact upon homing, correlating with the results observed in Figure 7. Interestingly, though Stamper-Woodruff assays indicate that $\alpha_4\beta_7$ may play a role in lymphocyte binding to HEV in CLN and PRLN, FIB 30 mAb showed

no blocking of short term lymphocyte homing in these tissues, though it did block homing to the PP, MLN, and NALT. Results from our *ex vivo* binding studies revealed that $\alpha_4\beta_7$ interactions with diffuse VCAM-1 expression in PRLN played an important role in lymphocyte binding. However, the sectioning of the node for the Stamper-Woodruff assay might provide access to the diffuse VCAM-1, allowing the cells to bind around, but not actually to, the HEV.

Analysis of long term lymphocyte retention of CONALT lymphocytes (Table 8) after 24 hours again revealed that a significantly higher percentage of CONALT GFP⁺ lymphocytes were retained in SMLN, and PRLN rather than in NALT and PP ($p = 0.03$). As observed following short-term lymphocyte homing, a smaller percentage of lymphocytes was retained in CLN when compared to the other nodes. Correlating with the data shown in Figure 7, MEL 14 significantly blocked the majority of lymphocyte retention in CONALT (Fig 11 B; $p < 0.001$), while FIB 30 mAb had little to no effect on lymphocyte retention. These results also showed that treatment with FIB 30 mAb significantly reduced the percentage of GFP⁺ lymphocytes retained within CLN ($p = 0.03$) indicating a possible role for $\alpha_4\beta_7$ binding to the diffuse MAdCAM-1 expressed in the follicles of this tissue. Surprisingly, however, treatment with FIB 30 mAb did not reduce lymphocyte retention in the PRLN, where it appears likely that $\alpha_4\beta_7$ can bind to diffuse VCAM-1. The ability FIB 30 mAb to block lymphocyte retention in PP, which also expresses diffuse MAdCAM-1, was reduced as well. These results suggest FIB 30 might have limited ability to remain bound to $\alpha_4\beta_7$ and retain its activity through 24 hours. In contrast, the MEL 14 mAb is retained on the surface of the lymphocytes

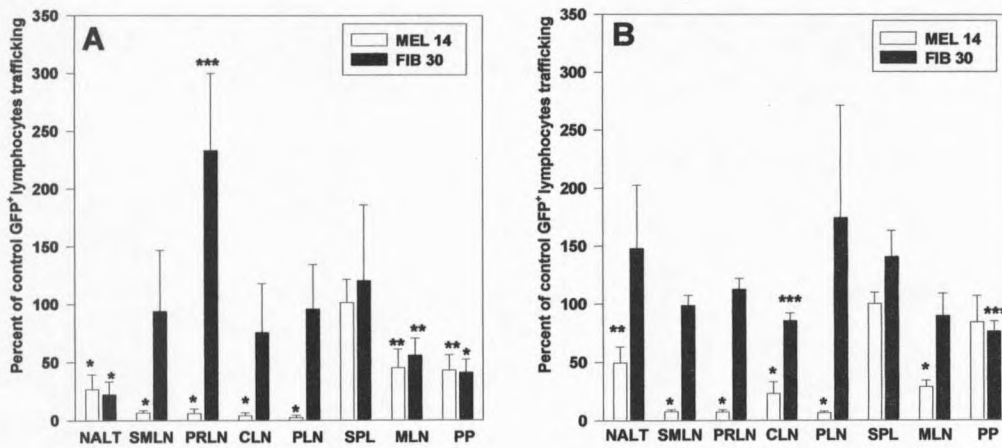


Figure 11. Treatment with an anti-L-selectin Ab reduces lymphocyte homing and retention in CONALT. CONALT lymphocytes were derived from GFP⁺ donor mice and treated with either MEL 14 or FIB 30 mAb, and then injected into recipient C57BL/6 mice. The results of five experiments (mean \pm SEM) are depicted as the percentage of GFP⁺ lymphocytes that trafficked to each tissue in the presence of IgG2a control antibody at (A) 4 hours and (B) 24 hours post-injection. * $p < 0.001$ ** $p \leq 0.01$ *** $p = 0.03$.

throughout 24 hours and continues to prevent lymphocyte trafficking at this time. With the results from our *ex vivo* lymphocyte binding assays, these data indicate the primary importance of L-selectin for trafficking to the mucosal LN of the head and neck, though the CLN appears to rely on some mucosal addressin-homing receptor interactions.

Implications of variable expression of MAdCAM-1 among CONALT

It has been demonstrated that the CONALT, mucosal inductive sites for the upper respiratory tract and oral cavity, express primarily a peripheral addressin phenotype much like the NALT (189). However, there is variability in the percentage of HEV co-expressing MAdCAM-1 and PNAd between the CLN, SMLN, and PRLN, with the CLN expressing the most mucosal addressin phenotype, while the PRLN expresses almost exclusively peripheral addressin. Though naive lymphocyte binding and trafficking in these LN is mediated primarily by PNAd-L-selectin interactions, some MAdCAM-1- $\alpha_4\beta_7$ mediated lymphocyte binding occurs in the more mucosal CLN, which also expresses intense staining of extravascular MAdCAM-1, and little to no staining of diffuse VCAM-1. In contrast, the more peripheral PRLN appears to express high levels of extravascular VCAM-1 that can bind $\alpha_4\beta_7$, but does not express diffuse MAdCAM-1. In addition, the results of this study show that > 90% of lymphocytes in the CONALT express L-selectin. In contrast, while the majority of B lymphocytes expressed $\alpha_4\beta_7$, less than half of the T lymphocytes expressed this integrin. Also, the majority of lymphocyte trafficking to the CONALT is mediated by L-selectin. Collectively, these results provide evidence for the primary role of peripheral addressin-homing receptor interactions in lymphocyte

trafficking to CONALT and suggests a role for MAdCAM-1- $\alpha_4\beta_7$ interactions in retention in CLN, but not PRLN or SMLN.

Since the CLN drain the SMLN, and both drain the NALT and the nasal submucosa (60, 86, 87), it might be expected that these LN would share a similar addressin phenotype with each other and with the NALT. Instead, more than double the percentage of HEV in the CLN co-expressed MAdCAM-1 (24%) when compared with the percentage of co-expressing HEV in the SMLN (10%). In addition, both of these LN expressed significantly fewer MAdCAM-1 positive HEV compared to the NALT, where 60% of the HEV expressed both MAdCAM-1 and PNAd (189). Finally, lymphocyte homing studies indicated that CONALT lymphocytes selectively traffic back to CONALT, rather than to the NALT. However, it is also possible that these LN, while they share common pathways of lymphocyte drainage, may not necessarily require the same addressin profiles on their HEV to allow these tissues to mediate cell trafficking from distal mucosal tissues. For local immunity, Ag will drain from the nasal submucosa, the NALT, the oral cavity, or the skin of the head and neck to the various CONALT, whose unique addressin profiles might then support the trafficking and retention of selective lymphocyte subsets to each LN where B and T cells can then activate and assume a memory phenotype. It is also possible that the expression of PNAd by nearly all HEV in the CLN and SMLN, and PNAd-L-selectin mediation of almost all naive lymphocyte binding may serve an important function in these LN. Expression of PNAd by the LN that drain and collect Ag from the nasal passages might allow for the trafficking of naive lymphocytes, almost all of which express L-selectin. Thus, the

chances that a naive lymphocyte will encounter and react to nasally-introduced Ags are greatly increased.

Though little initial lymphocyte binding is mediated through MAdCAM-1- $\alpha_4\beta_7$ interactions, MAdCAM-1 might indeed be necessary for trafficking of some lymphocyte subsets into the CONALT. Because 5-24% of HEV in CONALT co-express MAdCAM-1 and PNAd, it seems likely that MAdCAM-1 provides the glycoprotein backbone for the carbohydrate PNAd expression (101, 119), thereby binding L-selectin⁺ lymphocytes. Results from our Stamper-Woodruff assays showed that in the CLN, which expressed a more mucosal phenotype with 30% of its HEV expressing MAdCAM-1, treatment with FIB 30 mAb and MECA 367 mAb significantly reduced lymphocyte binding. $\alpha_4\beta_7$ interactions with diffuse MAdCAM-1 expression might mediate lymphocyte retention in CLN since the number of lymphocytes capable of homing was reduced by treatment with the FIB 30 mAb.

The "more mucosal" addressin profile expressed by CLN may allow it to perform a unique role as an inductive site in the head and neck. Functionally, while CLN is thought to drain most of the LN of the head and neck (60), the deep CLN have been shown to play an important role in the induction of immunity in the central nervous system, as Ags injected into the brain subsequently drain to the CLN, and removal of the CLN ablates experimental autoimmune encephalomyelitis (88, 89, 94). Located deep within the muscles of the neck, the CLN serve ideally as central nodes, and most likely play an important role in the induction of immunity in the CMIS. Consequently, the expression of MAdCAM-1 on its HEV might allow for selective trafficking of $\alpha_4\beta_7^{\text{high}}$ lymphocytes

from other mucosal sites (149, 151) that might react to antigen that has drained from the central nervous system.

In contrast to CLN and SMLN, the PRLN appear to function as more of a peripheral type of LN. Though located in close proximity to the parotid gland, the PRLN drain the skin of the head and neck (60, 78) and induce primarily systemic IgG responses (78). Our results strengthen these observations, as the PRLN predominantly display PNAd and bind naive lymphocytes primarily through PNAd-L-selectin interactions. Surprisingly, in the PRLN, treatment with FIB 30 mAb reduced naive lymphocyte binding by approximately 40%, but the effect of MECA 367 mAb was negligible. Subsequent treatment of PRLN HEV with MVCAM.A mAb reduced binding by approximately 50%. It has been shown that both $\alpha_4\beta_7$ and $\alpha_4\beta_1$ bind to VCAM-1 expressed by dendritic cells and macrophages (111, 147, 185). Since blocking of β_1 had no effect on binding, it seems likely that the extravascular VCAM-1 in the PRLN mediates *ex vivo* lymphocyte binding in close proximity to, but not on, the HEV through interactions with $\alpha_4\beta_7$. This result was supported by the data from our *in vivo* homing studies, which revealed that treatment with the FIB 30 anti- β_7 mAb had no effect on lymphocyte trafficking to this node, while treatment with an anti-L-selectin mAb almost completely blocked homing. Therefore, the PNAd expressed on the HEV of the PRLN may result in the trafficking of primarily L-selectin⁺ lymphocytes to this node, while high extravascular expression of VCAM-1 contributes to the retention of lymphocytes.

Finally, these results support the notion that MAdCAM-1- $\alpha_4\beta_7$ interactions may be considered to be predominantly intestinal rather than mucosal. Though the HEV of the

CONALT express MAdCAM-1, most cell binding, as well as lymphocyte homing and retention, was mediated through PNAd-L-selectin interactions. Indeed, MAdCAM-1- $\alpha_4\beta_7$ interactions do not play a major role in homing of lymphocytes in the lung or pulmonary tissues (124, 152-154), nor are they necessary for naive lymphocyte binding to NALT (189). The PNAd expressed on the HEV of the CONALT, the mediation of binding through PNAd-L-selectin interactions, and the high percentage of L-selectin⁺ lymphocytes in these tissues provides further evidence that peripheral addressins and homing receptors are important in lymphocyte trafficking to and from the nasal passages and the salivary glands. This also suggests that pathways of lymphocyte homing to these tissues differ greatly from those observed in the gut. Collectively, this would imply that not all mucosal tissues phenotypically or functionally behave as intestinal tissues, and the variability among mucosal tissues to effect distal mucosal immunity may be dictated by the residing addressin phenotype.

CHAPTER 5

MAdCAM-1 EXPRESSION IS INCREASED ON HEV AND DENDRITIC CELLS OF CT IMMUNIZED NALT

Introduction

Nasal-associated lymphoid tissue (NALT) induces strong immune responses following nasal immunization. Since i.n. immunization represents an attractive route for vaccination (20, 21, 27, 28, 36), it is important to determine the mechanism for the trafficking of lymphocytes to and from this site. As a mucosal inductive site, NALT has often been compared with the intestinal PP (26). However, our previous work (189) has shown that unlike the PP, where MAdCAM-1- $\alpha_4\beta_7$ interactions mediate lymphocyte homing to this tissue, lymphocyte trafficking to naive NALT is mediated primarily by PNAd - L-selectin interactions.

Changes in addressin expression might occur during an immune response in NALT. Studies have shown that MAdCAM-1 is up-regulated in inflamed intestinal tissue (112, 148, 193), inflamed pancreas (194), and in CNS during chronic experimental allergic encephalitis (195, 196). In addition, expression of the MAdCAM-1 ligand, $\alpha_4\beta_7$, may be necessary for intestinal memory cells to traffic to sites of inflammation (149-151, 197). In contrast, memory lymphocyte homing to peripheral sites (157-159) as well as the lung (198) appears to be mediated by PNAd-L-selectin interactions. It is unknown, however, whether lymphocyte homing to the immunized NALT will continue to be mediated primarily through peripheral addressin - homing receptor interactions, or if

mucosal immunization will result in an upregulation and corresponding increase in functionality of MAdCAM-1.

Recently, it has been determined that non-HEV-associated MAdCAM-1 is up-regulated in immunized PP (145). This diffuse expression of addressins has also been noted in PLN, where non-vascular VCAM-1 has been observed in germinal centers (147). More importantly, diffuse MAdCAM-1 and VCAM-1 found in germinal centers has proven to be functional, as lymphocytes bind specifically via expression of $\alpha_4\beta_7$ or $\alpha_4\beta_1$. Expression of diffuse MAdCAM-1 in GC and in the SED of PP has been shown to correlate with the presence of DC in these areas (145).

All DC can be identified by their expression of CD11c (199). Recently it has been reported that these DC can be subdivided into three groups based upon expression of various cell surface antigens, and dynamics within the lymphoid tissue (200), though little is known about their location or roles within the lymph node. It has also been reported that two subsets of dendritic cells can be found in the PP (57, 201). These subsets can be classified as sub-epithelial dome (SED) dendritic cells, characterized by CD11c⁺/NLDC-145⁻ phenotype, and interfollicular region (IFR) dendritic cells characterized by a CD11c⁺/NLDC-145⁺ phenotype. The SED layer of epithelial cells is thought to play a specialized role in the presentation of antigens that are captured from the intestinal LP. Given that NALT shares structural similarities with the PP, including a layer of M cells, it is likely that these two subsets of dendritic cells will be identified in the NALT as well, though it has yet to be determined if the diffuse MAdCAM-1 expressed in NALT also associates with DC localization.

In the following studies, we show that the expression of MAdCAM-1 by HEV of the NALT is up-regulated by immunization with CT, which induces a potent Th-2 type response in mucosal tissues (172, 202). The functionality of the addressin is increased as well, since blocking with anti-MAdCAM-1 antibodies reduces the ability of lymphocytes to bind to immunized NALT. Finally, we have shown that the expression of non-HEV-associated MAdCAM-1 co-localizes with N418⁺ DC in the SED of immunized NALT, providing further evidence for the role of addressin expression by antigen-presenting cells in mucosal inductive sites.

Results and Discussion

The percentage of HEV expressing MAdCAM-1 is increased in CT immunized NALT

Since MAdCAM-1 has been shown to be up-regulated in mucosal sites following immunization (112, 148, 184) we questioned whether the inductive site for the nasal passages, the NALT, which in a non-immune state expresses primarily PNAd, would show a similar response after CT immunization. Mice were nasally immunized with 5 μ g CT, then boosted 7 and 14 days post initial immunization with 2.5 μ g CT. NALT were removed at various days post-immunization, stained for expression of PNAd and MAdCAM-1 via immunofluorescent or immunohistochemical staining, and HEV expressing MAdCAM-1 were enumerated.

Our results show that by 10 days post-immunization, a significant increase in the number of MAdCAM-1 expressing HEV occurred in NALT (Figure 12, Table 9). Whereas naive NALT co-expresses MAdCAM-1 and PNAd on 60% of its HEV (189),

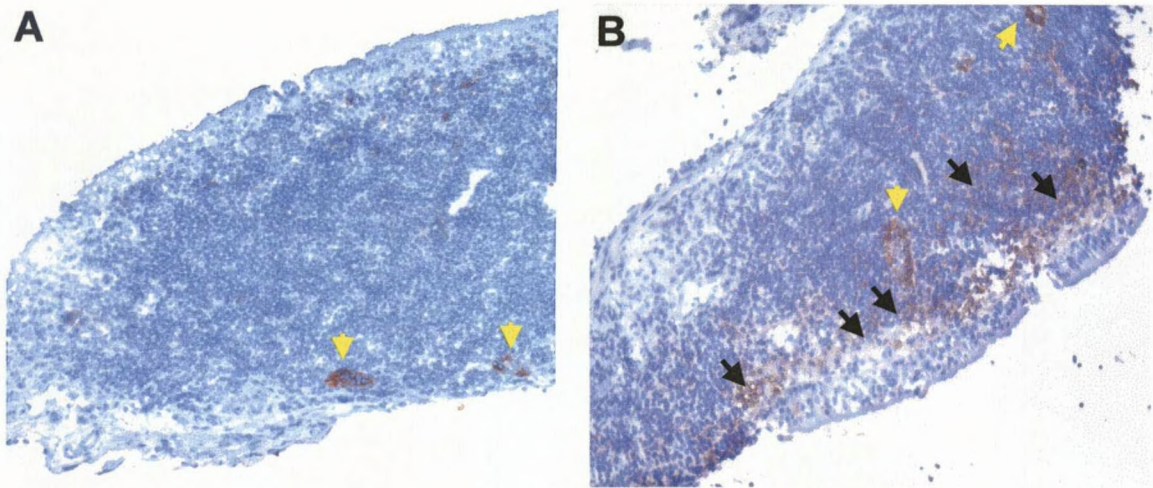


Figure 12. MAdCAM-1 expression is increased on HEV (yellow arrowheads) and in stromal cell areas (black arrows) in 10 day CT-immunized NALT. Non-immune (A) and 10 day CT-immunized (B) NALT sections were stained with MECA 367, and color was visualized by AEC substrate and counterstain with hematoxylin.

Table 9. Increase in the number of HEV expressing MAdCAM-1 in CT immunized NALT^a

Days post CT immunization	Percentage of HEV expressing MAdCAM-1	number of NALT analyzed ^b
0	57.8 ± 2.5	16
1	66.0 ± 1.9	4
3	71.2 ± 10.6	3
5	73.3 ± 7.2	3
10	78.9 ± 6.2 ^c	12
14	73.2 ± 1.8	2
21	91.6 ± 8.4	2

^aMean values are expressed as the percentage of HEV expressing MAdCAM-1, either with PNAd or alone/total number of HEV/node

^b 7 - 10 HEV are found per NALT

^c $p < 0.05$

the number of MAdCAM-1 positive HEV in 10 day post-immunized NALT increased to nearly 80% ($p < 0.05$). The number of HEV expressing MAdCAM-1 continued to increase, and by day 21, an average of 90% of HEV were stained by the MECA 367 mAb. The majority (>99%) of HEV counted in these studies co-expressed MAdCAM-1 with PNAd; very few HEV expressed MAdCAM-1 alone (data not shown).

Increased MAdCAM-1 expressed by immunized NALT HEV is functional

We next performed a Stamper-Woodruff *ex vivo* assay in order to determine if the MAdCAM-1 expressed by the HEV in immunized NALT had an increased function in the binding of lymphocytes to this tissue. MLN lymphocytes were rotated over frozen NALT sections in the presence of isotype control antibodies, anti-L-selectin mAb MEL 14, anti- β_7 mAb FIB 30, anti-PNAd mAb MECA 79, or anti-MAdCAM-1 antibody MECA 367. Comparison of *ex vivo* assays performed on immunized NALT with the results obtained from our studies on normal NALT revealed that MECA 367 and FIB 30 showed increased blocking of lymphocyte binding to HEV, while the ability of MECA 79 and MEL14 to block binding was reduced (Figure 13). In these experiments, both MECA 79 and MEL 14 treatments completely blocked lymphocyte binding to naive NALT, while MECA 367 reduced binding by approximately 40%. In immunized NALT, treatment with MECA 367 reduced binding to 50% of control. In addition, the MEL 14 mAb, which blocks 95% of cell binding in normal NALT, blocked approximately 85% of binding in immune NALT. The most striking difference between normal and immune NALT, however, was the effect of the FIB 30 antibody, which did not block lymphocyte

binding to naive NALT at all, but reduced binding to immunized NALT by 40% (Figure 13).

When the number of cells binding to HEV was compared between normal and immunized tissue, we found that almost 24 times more lymphocytes bound to immunized NALT HEV than normal NALT HEV in the presence of MEL 14 (Figure 14). The number of cells binding to tissue in the presence of MECA 79 in immunized tissue was two-fold higher than that of cells binding in normal tissue. In addition, the number of lymphocytes binding to immunized NALT with treatment of FIB 30 was decreased by one-fold from the number of lymphocytes binding to normal NALT, indicating additional blocking by this antibody. As evidenced by the increased ability of FIB 30 to block lymphocyte binding and the decrease in the ability of MEL 14 and MECA 79 to block binding to immunized NALT, the MAdCAM-1 expressed by HEV in immunized NALT tissue is functional.

Diffuse MAdCAM-1 staining correlates with N418⁺ DC cell staining

In addition to an increase in the number of HEV expressing MAdCAM-1 on the HEV of CT immunized NALT, we also observed an increase in the intensity of staining of diffuse MAdCAM-1 both in follicular regions, as well as in the SED region of immunized NALT (Figures 12 and 15). Since it has been reported that MAdCAM-1 may be expressed by DC in the follicle of the PP (145), we investigated whether diffuse expression of MAdCAM-1 correlated with co-localization of DC subsets.

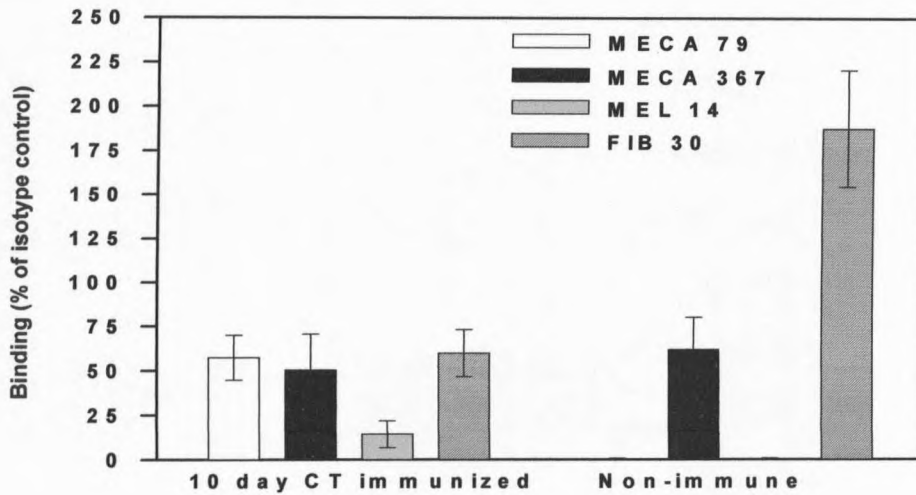


Figure 13: MEL 14 and MECA 79 mAb have decreased blocking ability in 10 day CT-immunized NALT. MLN lymphocytes ($10^7/\text{ml}$) were treated with $50\mu\text{g}/\text{ml}$ of anti-L-selectin mAb MEL14, anti- β_7 mAb FIB 30, anti-MAdCAM-1 mAb MECA 367 or anti-PNAd mAb MECA 79, or purified isotype-matched negative control mAb. The average number of lymphocytes bound/HEV in each node was determined, and results are expressed as the percentage of cells bound in the presence of isotype-matched control Ab. Results are the mean of three experiments \pm SEM.

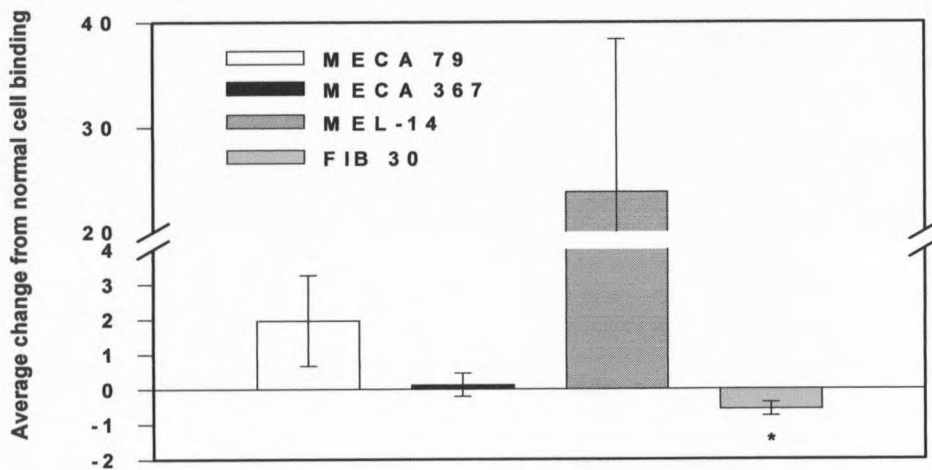


Figure 14: The ability of MEL 14 and MECA 79 mAbs to block naive lymphocyte binding to immunized NALT HEV is decreased. The average number of cells binding to HEV in normal NALT in the presence of FIB 30, MEL 14, MECA 79, or MECA 367 was set as a standard, while the number of cells binding in the presence of the same mAb in immunized NALT is expressed as x times the standard number of cell binding. More cells bind in the presence of MEL 14 and MECA 79 mAbs, while fewer cells bind in the presence of FIB 30 mAb. Results are the mean of three experiments \pm SEM.

In order to identify DC subsets that were present in NALT, we performed immunoperoxidase stains using mAb N418, which identifies CD11c⁺ DC located in both SED and interfollicular (IFR) regions, as well as mAb NLDC-145, which binds to IFR DC only. Our results showed that both SED N418⁺ and IF NLDC-145⁺ DC were present in NALT (Figure 16). More importantly, N418 staining of SED DC appeared to correlate with expression of diffuse MAdCAM-1 in the SED region of the NALT (Figure 15).

To further determine if N418⁺ SED DC were indeed expressing MAdCAM-1, we next performed a double immunofluorescent stain using N418 and MECA 367. Results from these experiments revealed that in non-immune NALT, N418⁺ DC and diffuse MAdCAM-1 staining was observed with some co-localization of MECA 367 and N418 Abs (Figure 17 left panel). These results indicate that some diffuse MAdCAM-1 present in the SED region of non-immune NALT was expressed by DC while some cells expressing MAdCAM-1 did not stain with the N418 Ab. Staining of CT immunized NALT tissue 10 days post-immunization showed an increase in staining of MAdCAM-1 and definite co-localization of N418 and MECA 367 staining (Figure 17 right panel), indicating that some immunized SED DC expressed MAdCAM-1. However, some diffuse MAdCAM-1 staining was again observed independent of N418⁺ cells, suggesting that expression of diffuse MAdCAM-1 in the SED region of the NALT may not be entirely dependent upon DC. Co-localization of diffuse MAdCAM-1 and DC markers was not observed in GC.

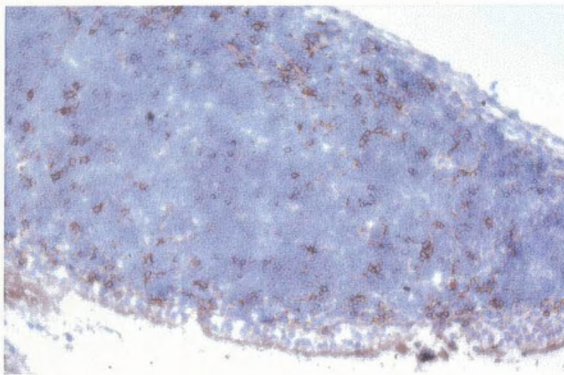
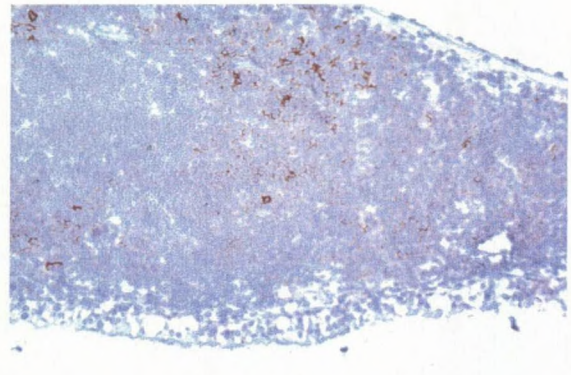
**N418****NLDC-145**

Figure 15: Two subsets of dendritic cells are present in immunized NALT. 10 day CT-immunized NALT was treated with N418 mAb, which recognizes DC in SED and GC regions, and NLDC-145, which binds to DC in GC regions. Ab binding was visualized with AEC substrate and counterstained with hematoxylin.

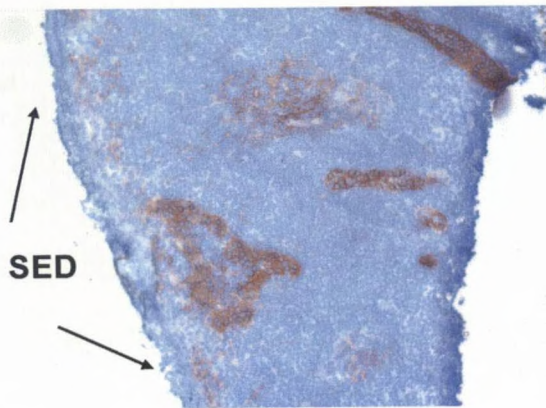
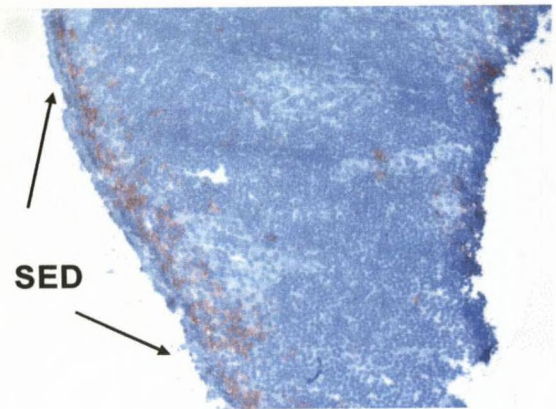
**MAdCAM-1****N418**

Figure 16: Expression of MAdCAM-1 and SED DC appear in subepithelial dome region (SED) of 10 day CT-immunized NALT. Anti-MAdCAM-1 mAb MECA 367 binds to HEV, SED region, and GC, while N418 mAb binds to DC in the SED region. Ab binding is visualized by AEC substrate and hematoxylin counterstain.

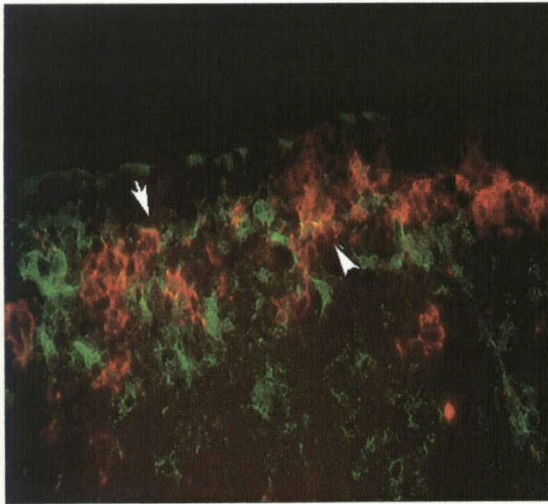
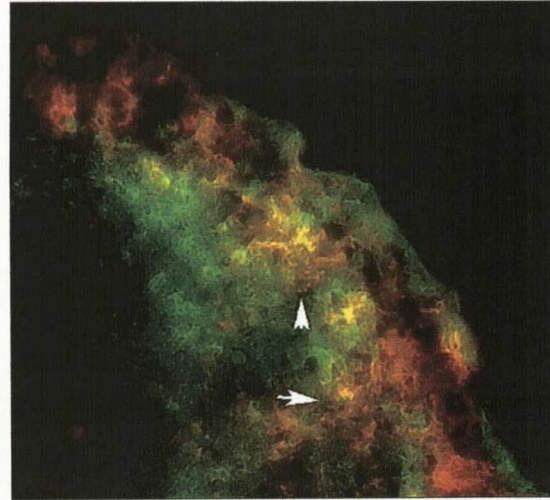
**Normal****10 day CT immunized**

Figure 17. N418⁺ DC co-localize with MAdCAM-1 staining in 10 day CT immunized NALT. NALT were stained with biotinylated MECA 367 mAb followed by SA-FITC (green) and N418 mAb followed by PE labeled anti-hamster secondary Ab. Co-localization of Abs is indicated by white arrowheads

MAdCAM-1 expression on HEV and DC is dynamic

These studies have shown that although PNAd is predominantly expressed on HEV of naive NALT and naive lymphocyte binding to this tissue is primarily mediated by L-selectin interactions (84), mucosal immunization induces an increase in the number of NALT HEV expressing MAdCAM-1. The MAdCAM-1 expression on HEV has an increased function, as *ex vivo* lymphocyte binding to NALT immunized HEV was decreased by treatment with anti-MAdCAM-1 and anti- β_7 mAbs. We also observed intense staining of non-HEV associated diffuse MAdCAM-1. In addition, we have identified co-localization of diffuse MAdCAM-1 expression with N418⁺ DC in the SED region of the NALT.

MAdCAM-1 is upregulated on inflamed intestinal tissue in murine models of colitis (112, 148, 193), as well as in pancreas in mouse diabetic models (194), and in CNS during experimental autoimmune encephalitis (195, 196). This increase in expression was noted on flat-walled endothelial venules located within intestinal lamina propria and stomach, in pancreatic islets, and on epithelial cells in the choroid plexus rather than on HEV located in an organized lymphoid structure. The MAdCAM-1 expressed in these inflamed tissues plays an important role in the recruitment of memory T lymphocytes to these sites, as treatment with MECA 367 and anti- β_7 mAb inhibits trafficking and reduces inflammation (148, 203). It is possible then, that the increase in NALT HEV expressing MAdCAM-1 following CT immunization might provide a mechanism for the recruitment of antigen-specific memory T and B lymphocytes to the NALT. However, all HEV expressing MAdCAM-1 also expressed PNAd, indicating that

there may still be a role for peripheral addressin-L-selectin interactions in memory lymphocyte trafficking.

Blocking of lymphocyte binding by MEL 14 varied greatly between normal and immunized NALT. In the immunized NALT, nearly 24 times more lymphocytes bound to HEV in the presence of this antibody than on naive NALT. In addition, there was a subtle increase in the ability of the FIB 30 and MECA 367 Ab to block lymphocyte binding to immunized versus normal NALT. Therefore, it is likely that some lymphocyte binding to immunized NALT is mediated through $\alpha_4\beta_7$ -MAdCAM-1 interactions. However, the majority of lymphocyte binding to HEV of immunized NALT appeared mediated by PNAd-L-selectin interactions. Together, these data suggest that though the increased MAdCAM-1 expression on HEV has some function, there is still a significant role for peripheral addressin-homing receptor interactions in lymphocyte trafficking to immunized NALT.

We also identified an increase in the diffuse expression of MAdCAM-1 in the follicular and SED regions of the NALT after CT immunization. Double immunofluorescent staining revealed that in immunized and naive NALT, some MAdCAM-1 expression co-localized with N418⁺ staining of DC in the SED region. Expression of MAdCAM-1, and co-localization of MECA 367 and N418 mAb were more pronounced in immunized NALT. Diffuse MAdCAM-1 in normal NALT, as well as some MAdCAM-1 in immunized NALT were expressed by reticular cells other than N418⁺ DC. This is in direct contrast to the results reported by Szabo, *et al* (145), who stated that DC in the GC of inflamed PP and PLN expressed MAdCAM-1. However, no

